Rebuttal to reviewer 1

Reviewer comments R1:

Review of the manuscript „A comparison of two astronomical tuning approaches for the Oligocene - Miocene Transition from Pacific Ocean Site U1334 and implications for the carbon cycle“ by Helen Beddow et al.

Dear Authors,

With great interest, I have read your manuscript. You review the Oligocene-Miocene boundary magnetic and cyclostratigraphic time scale, and test it by tuning two proxies (CaCO3, d13C) from IODP Site 1264. Using these tuning options, you test their consistency with sea floor spreading rates. Finally, your approach provides astronomically tuned chron ages and implications for the Carbon cycle This manuscript has a stratigraphic and carbon cycle focus and discusses the effect of orbital tuning for time scales and carbon cycle interpretations, which are without doubt relevant for paleoceanographic and paleoclimatic studies. You propose an orbitally tuned magnetic polarity time scale for the relevant time interval, which is relevant and a valuable outcome of your study. All over the manuscript is clearly structured and written. High quality figures complement the text in a logical way. The manuscript is in my opinion clearly in the scope of Climate of the Past. A revised version of this manuscript suits the scope of CP, and I recommend publication after below mentioned clarifications/revisions. I hope the comments below help to make your manuscript more clear and relevant to a wide readership. It is clearly meant as constructive

A small correction: we have used IODP Site U1334 instead of ODP Site 1264.

‘General comments’

To be honest, it took me quite some reading to realise why you use the approach presented in your manuscript, and I ask you to clarify this earlier and clearer. You compare tuned ages, based on CaCO3 and d13C records. I was wondering what is your initial argument for using d13C as signal for in-phase tuning? Several studies have shown that this assumption may be problematic in the Neogene and Oligocene (as you also state), and that d13C signals are time-delayed relative to other proxies and eccentricity. Personally, I would expect a delay of this signal relative to physical and/or chemical proxy data. Importantly, Liebrand et al., (2016) demonstrated that at Site 1264 the d13C signal has a ~5-10 kyr time offset relative to CaCO3, therefore it is hard to understand why you would knowingly use an offset signal as tuning target.

The main reasons to use $\delta^{13}C$ for tuning is (1) to test if the generally strong expression of the 405 ky eccentricity cycle in benthic $\delta^{13}C$ yields similar/comparable ages to tuning approaches based on lithological proxies, and 2) to independently test the (previously presumed) phase lag of the benthic $\delta^{13}C$ signal w.r.t. eccentricity with independent

evidence that is free from tuning assumptions. The spreading rates provide independent evidence that the lag of the benthic isotopes is a real feature and that tuning to the 405-ky cycle in benthic foraminiferal $\delta^{13}C$ does not yield ages that are in agreement with spreading rates.

Please make this choice clearer early in the manuscript (as I read the manuscript parts of your reason are rather hidden around lines 335-343). Your intention to test phase relations and their stability regarding the phase comes rather late in your manuscript. In any case it may need to be clarified that one tuning option is rather artificial and only used as test, with the expected outcome that it will not be good/valid.

With the knowledge of hindsight, we agree that the $\delta^{13}C$ tuning option seems rather artificial. However, by showing the implications of this tuning option for spreading rates, we can rule it out completely. For the sake of argument (i.e., comparing tuning options and provide independent evidence for chron ages and leads and lags in the climate-carbon cycle system) it is best to keep an open mind about both tuning options, until we reach the discussion and are able to discuss the implications of these tunings. We note that, in the introduction, we clearly state the aim of the research (see last paragraph of the introduction). Sentence beginning with "We evaluate…".

According to your Fig. 7, and the preferred age model, a short interval around 23.1-23.1 Ma experiences sedimentation rates two times as high as previously and afterwards. In my opinion, the exact doubling for one 100 kyr cycle mean that actually two cycles were combined. Having less experience with this specific dataset than you, in my opinion the data structure would allow such an interpretation in this interval, also when considering eccentricity being expressed as precession amplitude. Please discuss this option (or why this may not be the case) in the manuscript.

The preferred age model, supported by spreading rates, is the $CaCO_3$ tuned age model (Fig. 6) and not the $\delta^{13}C$ tuned age model (Fig. 7). A brief spike in sedimentation rate near 23.1 Ma (Fig. 7e) is indeed an artefact of misinterpreting two 100-kry cycles as one. The spreading rate history clearly rules this option out. Unfortunately, we are not able to use precession, or its amplitude, as it is not well expressed in the data. We have reordered the discussion and the age model evaluation section (see also comments to R2). Both age model options are now discussed in more detail; including discussion on sedimentation rates, phase assumptions and cyclostratigraphic interpretations.

I would propose to include a more thorough discussion on what the age model differences mean for phase relations, also in context of the recent manuscript by D. Khider 'The role of uncertainty in estimating lead/lag relationships in marine sedimentary archives: A case study from the tropical Pacific: Lead/Lag uncertainties' (Khider et al., n.d.). Your d13C tuning leads to an out-of-phase relationship (lines) of the d13C signal. This is stated, but not discussed. Please discuss why this may be the case, and what it tells about reliability of the signal and tuning.

An error had crept in Fig. 5 depicting the phase relationships. We have updated the figure and text that discusses the phase relationships. The Khider reference is only partially relevant, because they study the last three glacial, which are much better constrained in time compared to the Oligo-Miocene records. We do refer to Khider now, to highlight potential avenues for future research.

Apparently, you use MS data to derive CaCO3. Is there any reason why you do not directly use the MS for tuning then? This is not clear to me, so please clarify this, and demonstrate that the original MS data also supports your conclusions and these signals are in phase when tuned. Results/Figures may go to Supplements. I think demonstrating this will strengthen your manuscript and reasoning. Throughout the manuscript I propose to name the age model CaCO3/MS based, as it is more MS based than CaCO3 based to my understanding.

We have recomputed the conversion of MS into $CaCO_3$ and now use a linear transfer function. The signal structures are identical to one other and the tunings and phase calculations based on MS are similar to those of $CaCO_3$. We convert MS into $CaCO_3$ because ~90% (new improved conversion, using only coulometry data of the study interval) of the variance in the MS record is linked to $CaCO_3$. Variability in $CaCO_3$ estimates, however, is with most readers more strongly associated with lithology (and the processes underlying it: i.e. dissolution, dilution, productivity) than MS variability is. We have clarified the text in section 2.2 to better explain our choice for $CaCO_3$ est. over MS.

Although this is very recent literature, I think that discussing (Laurin et al., in press), their implications and your d13C results would be of advantage – though it would not change your results.

We have included Laurin et al and Khider et al. in the manuscript and reference list.

‘Specific comments
Below you find further remarks. Addressing these would improve your manuscript in my opinion.

Line 33: “correct”: Are you sure one of these is correct in detail? Please rephrase.

We have rephrased this sentence.

Line 34: please explain “anomaly profiles”

We have rephrased this sentence.

39: C6Bn.1n–C6Cn.1: please provide rough age

We have added rough ages in parentheses.

58: Submitted? The paper without data in the reference list is published already,

https://www.clim-past.net/13/1129/2017/

We have updated this reference.

81: Here it may be useful to mention that the tuning process can introduce signals into datasets, as has been demonstrated by e.g. (Shackleton et al., 1995)

We discuss introducing spectral power in the data record in section 4.3.1. already. We have added a reference to Shackleton et al. 1995.

83-88: sentence is quite long, please phrase clearer.

We have rephrased this sentence.

144: SI units for MS refer to Volume. Later on you mention units/gram. Both can be correct, but please be careful not to mix the two, and use one consistent unit for the MS through the manuscript, ideally SI units.

We have changed "SI units" with "sensor values" [see: *Westerhold et al*., 2012a, *Pälike et al*., 2010], because our MS record refers to shipboard, whole-round core-logger MS values.

172: please state the re-sampling resolution (in depth or time, or both?)

We have added this information.

179: please specify details of the evolutive spectral method

We have added these details.

195: Please explain what survives here.

The Pacific plate survived. The Juan de Fuca plate was subducted. This has been clarified in the text.

207: 88%? In the Figure it looks like more than 90%, please check.

We have recomputed the $CaCO_3$ content of the sediment and adjusted the values in the text.

209: please explain 'CCSF'

We have explained CCSF in the main text of the manuscript.

220f: hard to see in Figures, please see comment on the Figures below.

See our reply below

223: Smaller? Weaker?

We have replaced “smaller” with “weaker”.

238 and elsewhere: significantly? At which confidence level? I cannot read the significance level from Figures, so please rephrase.

We have replaced “significant” with “strong”.

275: ‘smallest lag’ – relative to what?

We have added “with respect to orbital eccentricity”

304f: Tuning is expected to lead to increased power, see e.g. (Huybers and Aharonson, 2010; Shackleton et al., 1995).

We have added these references.

Generally 4.3. Please substantiate why you choose the d13C as tuning signal here. This information is rather hidden in lines 335-343.

This information was already given in this section. We state that $\delta^{13}C$ is one of two end-members (in terms of phase) for tuning [see, e.g. *Liebrand et al*, 2016., *Pälike et al.*, 2006a, 2006b]. Previous studies have implicitly assumed (correctly) that $CaCO_3$ often responds more directly to orbital forcing (though still nonlinearly) than the climatic components reflected by the O and C isotope systems. Here, we test this assumption, by showing that tuning to $\delta^{13}C$ does not yield satisfactory plate-pair spreading rate histories.

288: Ref to Fig. 6c: In Fig 6c the CaCO3 maxima are not really aligned with eccentricity minima (the dashed correlation lines are not consistent with this statement). Please make sure this is the case, I think this is a plotting issue, as data seem aligned.

The plot seems fine to us. The confusion is probably due to the filters of the ~110-ky signal that are sometimes slightly misaligned with the CaCO3 maxima that we manually selected. We have clarified the text.

296; Evolutive ? analysis: what kind of analysis?

We have added information wrt the kind of analysis.

366? More significant? (and 420f: ‘marginally significant’) Now, it is significant at 95% confidence or not? Maybe rather state ‘significant at higher confidence level?’ – if this is the case.

To prevent confusion with statistical significance, we have rephrased these sentences.

454: Can sedimentation rates give you information on a choice here as well? I propose to insert a brief statement/discussion on this.

We have added a brief discussion on the sudden increase in sedimentation rates here. Constant sedimentation rates are probably more likely.

484: these references are examples; please use 'e.g.'

We have added "e.g.".

506: 1264 à IODP Site 1264?

We have inserted "Site". IODP is already mentioned in the introduction.

516: … required to speculate? Please rephrase, as I do not think we need to speculate.

We have rephrased this sentence.

Figures: Please give correct units for the MS, "instrument units" are not reproducible.

Please see previous comment. We have replaced S.I. units with "sensor values" (according to IODP nomenclature). These MS records are measured on whole round multi sensor tracks and are measures per volume.

Figures: Please indicate which phase represents relative lag/lead

We have now indicated leads and lags with respect to eccentricity in Figure 5.

Fig 2a: high CaCO3 data seem to show less variability than low MS data – again, please note why you use CaCO3 data for tuning instead of MS data.

The low MS values are near the detection limit of the whole round sensor. The main features between the MS and CaCO3 are now identical due to the new linear transfer function that we applied. The conversion from MS to $CaCO_3$ did not affect the visual selection of tuning tie-points in the CaCO3 record, because these are all defined in $CaCO_3$ minima (i.e. MS maxima). We have described and clarified our choice for converting MS into $CaCO_3$ in section 2.2. of the main text.

Fig. 2b: R2 denotes the correlation between MS and CaCO3 or the fit between data and model? Please note that the high MS and low-CaCO3 part seems heavily influenced by a single high MS data point, which seems less representative than lower MS data points. Can this influence your results?

We agree that the correlation between MS and $CaCO_3$ was suboptimal. The entire MS record and coulometry data set for U1334 was used. We have replaced this conversion with one that only considers the data for our study interval, and that removes intervals from Site U1334 with very low and very high MS values. The R^2 value of the MS – coulometric $CaCO_3$ content measurements improved to 0,92. A very convincing relation between MS and calcium carbonate content, as is expected for the deep Pacific. Both MS and $CaCO_3$ estimates were considered during the tuning process and the y-axis conversion of MS values did not affect the tuned ages. In the main body of the text (section 2.2.) we discuss our choice of (new) transfer function.

Fig.3: please indicate the position of the OM boundary

We have now indicated the OMB.

Figs 3, 5: wavelet plots show a lot of irrelevant high-frequency noise. I propose to focus on relevant frequency ranges. This will make readers better able to reconstruct your statements in the manuscript.

Small correction: these are evolutive FFT analysis, not wavelet analysis. We prefer to also show the higher frequencies, because a lot of discussion in the literature is concerned with these cycles. By showing that obliquity and precession are not continuously present/strongly expressed, we visualize one of the main reasons why we tuned solely to the (stable) eccentricity solution.

Fig 5 nicely shows bifurcations of the 100-kyr cycle. These can be used to test phase relationships (Laurin et al., 2016). I encourage you to comment if the pattern is consistent with your assumption.

We have not looked into the details of how bifurcations of the ~110-ky cycle can shed further light on the individual 95 and 110-ky phase relationships to eccentricity. The main aim of this study is to identify the most suitable tuning signal curve and settle the ~110-ky tuning of the OMT interval.

Fig. 7 heading: … versus age.

We have added “age” in the figure caption.

References: I am aware of issues with proposing to cite references during the review process. Please see these as suggestions solely. For some cases, there are other papers which also point in the same direction. I clearly do not require you to cite this specific literature, but I ask you to consider their content, which in my opinion can improve your manuscript. Please decide yourself.

Huybers, P., Aharonson, O., 2010. Orbital tuning, eccentricity, and the frequency modulation of climatic precession. Paleoceanography 25. doi:10.1029/2010PA001952

Khider, D., Ahn, S., Lisiecki, L.E., Lawrence, C.E., Kienast, M., n.d. The role of uncertainty in estimating lead/lag relationships in marine sedimentary archives: A case study from the tropical Pacific. Paleoceanography 2016PA003057. doi:10.1002/2016PA003057

Laurin, J., Růžek, B., Giorgioni, M., n.d. Orbital signals in carbon isotopes: phase distortion as a signature of the carbon cycle. Paleoceanography 2017PA003143. doi:10.1002/2017PA003143

Liebrand, D., Beddow, H.M., Lourens, L.J., Pälike, H., Raffi, I., Bohaty, S.M., Hilgen, F.J., Saes, M.J.M., Wilson, P.A., van Dijk, A.E., Hodell, D.A., Kroon, D., Huck, C.E., Batenburg, S.J., 2016. Cyclostratigraphy and eccentricity tuning of the early Oligocene through early Miocene (30.1–17.1 Ma): Cibicides mundulus stable oxygen and carbon isotope records from Walvis Ridge Site 1264. Earth Planet. Sci. Lett. 450, 392–405. doi:10.1016/j.epsl.2016.06.007

Shackleton, N.J., Hagelberg, T.K., Crowhurst, S.J., 1995. Evaluating the success of astronomical tuning: Pitfalls of using coherence as a criterion for assessing pre-Pleistocene timescales. Paleoceanography 10, 693–697. doi:10.1029/95PA01454

Good suggestions. We have added these references to the text and reference list.

We would like to thank Christian Zeeden (R1) for his constructive comments.

Rebuttal to reviewer 2

Reviewer comments R2:

Review: Beddow et al.: "A comparison of two astronomical tuning approaches for the Oligocene-Miocene Transition from Pacific Ocean Site U1334 and implications for the carbon cycle" submitted to Climate of the Past.

General Comments:

Dear Beddow et al.,

The idea of using two different proxy series for astronomical tuning, and especially evaluating the differences between them in detail and the palaeoclimatological implications is excellent. I believe that the spirit of the paper, and the material presented, fall perfectly within the scope of the "Climate of the Past" journal. There are however some aspects that deserve further elaboration or better explanation to further improve the quality of the manuscript before publication. Below you can find my comments and suggestions.

Specific Comments:

Title:

"approaches" was confusing to me, first thought was that you used two different techniques to do the tuning, while you used two different signals/proxies (and corresponding phase relationships)from the same record. Suggest rephrasing of the title to make this clearer.

We have shortened the title and removed the word "approaches" from it.

Abstract:

Lines 25-30: confusing, you mention two different phase-assumption, but both are inverse and in-phase???

We have rephrased this sentence and clarified the difference between the two tuned age models.

L30-32: Not convinced that the two-end member idea is that well known to the average CP reader, and as such might not be clear in an abstract, more for later in the manuscript.

We have deleted this sentence from the abstract.

L33: what is ‘correct’?, maybe use something like ‘the most consistent with other data’, the most probable etc…

We have rephrased this sentence. See also comment R1.

Introduction:

L62: ‘tuning signal’ and ‘target curves’, while in L19-20 you use ‘climate proxy records and astronomical solutions’, to mean (as I understand it) the same thing. A consistent use of terminology might avoid needles potential confusion.

We use this terminology interchangeably. We have clarified this in the text.

Methods:

Not clear/obvious why you estimate CaCO3 from the MS signal. A motivation for this should be given in the introduction, so that the reader is not confused. Doesn’t one loose information, quality of data, by this extra step. The correlation is good, but not one-to-one.

We have not computed a new improved transfer function between MS and $CaCO_3$. See also comments to R1. We have clarified this in the text. See section 2.2.

Explain better sources data (place Wilson citation not optimal), and motivate selection of, plate-paired spreading rates. Maybe instructive to indicate those on your Fig. 1?

We have clarified the text, but not Fig.1. We refer readers interested in spreading rate histories to the study of Wilson. Here we focus predominantly on astronomical age calibrations and carbon cycle implications.

Results:

Presentation of the CaCO3 data is absolutely not clear, different numbers in diff figures, and the text. Adding stages in the plots would make reading much easier.
Not convinced by the mentioned higher frequencies in the CaCO3 record. Would be curious to see the MS spectra too. Could discuss the evolutionary spectrum also more, change over the boundary? Climate dynamics, changing sed rates?

We have updated the correlation between MS and $CaCO_3$, and the figures. The new linear correlation makes MS and $CaCO_3$ interchangeable in terms of cyclic patterns. Hence, their spectra are indistinguishable. We have also added periods to all figs (where relevant). The discussion of evolutive spectra has largely been revised. Also sedimentation rates are discussed in more detail. We discuss the climatic-carbon cycle dynamics in section 6.3.

Astronomical Tuning:

Side: Why are the sedimentation rate reconstructions for the CaCO3 done on the full eccentricity scale, and for the d13C on a higher resolution???

The $CaCO_3$ signal (as the MS signal) is predominantly a clipped (or skewed) signal with high $CaCO_3$ values dominating and a minimum $CaCO_3$ value every ~110 ky or so. Therefore, for this record, we visually selected tuning tie points in the $CaCO_3$ minima (i.e., MS maxima) only. The cycles in the benthic $\delta^{13}C$ are much more sinusoidal in shape. Therefore, we have visually selected tuning tie points in both ~110-ky cycle maxima and minima, which were selected in a Gaussian filter of the data on a polynomial age model through the GTS2012 assigned ages of the magnetic reversals. The higher number of tuning tie-points also affects the linear sedimentation rates computed based on the tie points. Section 4.3 explains the tuning procedures in much detail.

Side question. How is the tuning done? Manually extremum per extremum or with a software/script? Explain somewhere. Suggestion.

We tuned manually by visually selecting tie points in case of the $CaCO_3$ tuning and based on a ~110-ky filter in case of the $\delta^{13}C$ tuning. This is detailed in section 4.3.

In the d13C tuning this 50 kyr period will be close to 41 kyr, could this be an argument in favor of the d13C tuning (because tuning on the eccentricity makes the obliquity come out stronger, and you would expect an obliquity component no?)???

This could be an argument for the $\delta^{13}C$ tuned age model; however, there is no way of knowing. The test for the best astronomical age models, that we have constructed, uses independent evidence from plate-pair spreading rates. Assuming that obliquity must have had an affect on the global marine carbon cycle is more speculative, and not supported by the $CaCO_3$ tuned age model that is in best agreement with spreading rates.

L343: earlier on you mentioned the variability, sensibility of band pass filters to varying parameters, now you use the band pass filters to discuss phase relationships. How robust is this, or is there no problem? Also the phase relationships on Fig. 5 seem to be very sensitive to the used age models…

The exact position of filter minima and maxima is indeed dependant on the bandwidth of the filter. However, the filters depicted here were computed using broad bandwidths and qualitatively show the affect tuning has on the position of 405 ky minima and maxima in the benthic $\delta^{13}C$ wrt to those of eccentricity. The shift in these positions between the two age models is very robust. Unfortunately, the length of the time series was too short to compute phase evolution using, for example, Blackman-Tukey cross-spectral analysis (see e.g. Liebrand et al. 2017, PNAS). Therefore, we discuss the increased phase lag of the benthic $\delta^{13}C$ 405 ky cycle based on visual description, which is supported by filters.

And see ‘other comments’ too please.

See our reply below.

Discussion:

L443: I expected this discussion much earlier… it affects the interpretation of the previous paragraphs

Good point. We have reordered parts of the discussion and results in such a manner that we now first compare the to tuned age model to each other, and then use the plate pair spreading rate histories distinguish between the two tunings. Most of the content stayed the same, we now present the arguments in a more logical order.

L509-510: What might be the influence of the detrending (or not fully) of this d13C shift? Might it effect the BP filtering, be related to this peak in SR in C6Cn2r, add in the end an offset in age models??? Just an observation/thought…

The large positive shift in absolute benthic $\delta^{13}C$ values associated with the onset of the Oligocene-Miocene Carbon Maximum is also linked to the increase in phase lag of the 405 ky cycle. We have taken the bandwidths for filtering very broadly, which visualizes the observed phase lag. Detrending does not affect the phase lag of the 405-ky cycle in $\delta^{13}C$, because only periodicities >600 ky were removed using a notch filter.

Conclusions:

L525: 'insolation forcing' (actually also in your discussion), you tune on eccentricity, but eccentricity as such is only a very small component in the insolation term, eccentricity kicks in as amplitude modulator, non-linear feedbacks etc… should we be careful with the terminology?

Good point. We have added a sentence in the discussion to clarify this. All eccentricity signals in the U1334 records are of course a nonlinear response to the amplitude of precession (i.e. one of the two main insolation components that directly modulate seasonality). When we refer to insolation responses and eccentricity signals, the mechanistic link must be nonlinear and indirect.

References:

Not all consistent (for later, editing)

We have reviewed the references.

Missing in my opinion: Laurin et al., 2017, Paleoceanography

Suggestion, because very recent, Khider et al., 2017, Paleoceanography.

We have included these references in the manuscript.

Other Comments:

L24: again ‘tuning approaches’

We have rephrased “approaches” throughout the manuscript.

L58: submitted, in ref list as ‘in review’, published in CPD, be consistent.

We have updated this reference.

L62: ‘tuning signal’ and ‘target curves’, while in L19-20 you use ‘climate proxy records and astronomical solutions’, to mean (as I understand it) the same thing. A consistent use of terminology might avoid needles potential confusion.

We have clarified the text concerned with tuning signal and target curves.

L83-84: now you specify ODP and IODP, while you already referred to the concept of ‘Sites’ in the previous paragraph, maybe do this specification earlier in the manuscript.

We have corrected this in the text. The introduction of ODP is now moved forward, before we discuss the first sites.

L84: capital needed for ‘Middle Miocene’? is this an official term?

It is, but our use here is informal, hence the small letter.

L85: strange place to refer to Laskar et al., 2004, you didn’t specify the tuning sources for the previous paragraph, be consistent.

Indeed. We have removed this reference.

L88: be consistent in your referencing style, and make at the same clear which reference is for which record.

We have clarified the references here. 3

L89: remove ‘very’, suggestion

Removed.

L91: first time mentioning 110 and 405 kyr periods, maybe for the first time mention explicit link to eccentricity and explain why you use the number of ~110 kyr.

We now link these cycles to the stable eccentricity solution. The text concerned with tidal dissipation and dynamical ellipticity is moved to the discussion and removed from the introduction.

L95: what exactly was the first advantage? Clear cycles or good agreement?

See previous comments. The fact that eccentricity (in contrast to the obliquity and precession solutions) is stable is the first advantage. This has now been resolved.

L99: miss reference(s), how significant would that effect be (for the OMT)?

We have added references here. It could make a difference of up to a couple precession/obliquity cycles at 23 Ma. We refer the interested reader to *Lourens* et al. 2004.

L102: what about differences in age and duration estimates?

Good point. These are affected by tuning assumptions as well. We have clarified the text.

L114: also the CaCO3?

Yes. We have clarified this in the text.

L117: two end-member concept can use more explanation

We refer to section 4.3. for more explanation of this point. Here we briefly state what the reader will find in the manuscript.

L119: diff methods? More diff proxies (with corresponding phase interpretations), not my favourite formulation.

We changed "methods" for "proxies.

L120: now you talk about "records" (before: proxy or signal), I would prefer one consistent terminology. Mention explicitly, between brackets, which records.
See main comment about motivation for this CaCO3 estimate, and potential loose of quality of your data.

I think this is actually quite clear. Proxy signal, record, curve, target, solutions: these are all synonyms for time series. We have clarified these terms on a few occasions.

L148-153: not really 'Methodology'

We present this information here because we briefly want to explain what the $CaCO_3$ signal of the sediment may indicate. Understanding the tuning signal is important for the method of age model construction.

L160: “a”, typo?

Removed

L161: “and n” typo?

Removed

L172: resampled? What were the original and new resolutions? From Fig. 2 it seems that not all isotopic data has the same resolution, could this be important?

See also comments R1. We have clarified the text.

L173: small motivation for 6 m and 600 kyr? They don’t seem to represent the same amount of your signal???

These values are approximate, because the notch filter is Gaussian. The exact bandwidth did not crucially affect the detrending. We left the text as is.

L176: maybe mention that the bandwidths are mentioned in the fig captions.

We prefer the method section.

L178-179: window sizes and which method (e.g. FFT?) or evolutive analyses.

See comment R1. We have updated the text. Indeed FFT.

L182: Would make more sense to discuss the Wilson, 1993 paper in the introduction, where it is currently missing. Also is this paper the (original) source of your spreading rates?

We mention in the introduction that spreading rates have previously been used to constrain/check tuned age models. In our opinion, the introduction of the Wilson data is best presented here.

L184: missing “)”

We have removed the brackets altogether.

L184-186: sources rates for all Wilson paper? What is your motivation to select these four sets?

See comments R1. The text has been clarified wrt this point.

L199: which reversals?

We have added this information.

L206-207: the ranges on your plot 2a and 2b, and Fig 3 for CaCO3 and MS are different!!! How is this possible, highly confusing. Is one from core logging and others from discrete sampling? Needs to be clarified.

We have updated this plot, and now show the new, improved, correlation between MS and $CaCO_3$.

L208: below 70%? Also at other places? What is the point? Include the stages on the plots, this will make things much easier for all readers that might not be as familiar with the magnetostratigraphy as you are.

We have removed this sentence. We have added the Oligocene and Miocene Periods in Figure 3.

L213: where is the OMT on your figure?

See previous comment.

L215: refer to (sub)figure, where does this age come from?

Figure reference added. Age removed.

L216: is this higher amplitude variability so convincing? Often single points?

After the OMB clear 110 ky cycles are present. These consist of many data points.

L217: more positive or less? Lower values, reversed axis?

More positive values/higher values. The y-axes of the isotope plots are indeed reversed.

L224: where do you see these 1.83 and 2.8 c/m peaks in the CaCO3 record? I don't…

Agreed. Sentence removed.

L225: which high-amp cycles? Specify, be 100% clear.

We have clarified the text.

L228: any biostrat in addition to the magnetostrat?

No biostratigraphy.

L233: can refer to Table 1. Fig. 4

We have included these references.

L235: isn't evolutive a form of power spectrum?

Correct. We have removed the word "and" in between the two.

L238: what does significant mean?

See R1. "Significant" is replaced by "strong".

L240 CaCO3 est => different CaCO3 values ? never different on your figures…

We are not entirely sure what R2 means with this comment. We have updated Fig. 2b.

L245: I see your point, but here you took twice the same filter and is the different outcome because the different variations in both signals. Remove very.

We have deleted the sentence referring to filter bandwidth. This was out of place here. And removed "very".

L253: be consistent with your spelling of time(-)series

We have removed the dash

L256: reference to wrong figure, not Fig. 7

Changed into Fig. 5.

L257-261: repetition of intro, and this time with reference. Do once expanded in the intro.

We have chosen to remove it from the introduction and discuss tidal dissipation/dynamical ellipticity (and the implications for tuning) here.

L272: again, somewhere in the beginning you referred to different phase relationships???

Yes, both $CaCO_3$ and $\delta^{13}C$ are tuned in-phase with eccentricity, after multiplying the records with -1. However, both records contain different response times to eccentricity, resulting in different age models with differing leads and lags (i.e. exact phase relationships). To clarify the difference between leads and lags (which also contain phase information), and the 'broad correlation' between phases of cycles and how they correspond to one other (e.g. ecc max to $CaCO_3$ min), we have clarified the text.

L273-279: this would have been useful to read much earlier in the manuscript.

We do mention this in the last paragraph of the introduction. This is the section in which we further elaborate on this rationale.

L284-286: maybe shortly explain mechanistic link? Why higher CaCO3 in cooler period?

We now mention the mechanisms underpinning the $CaCO_3$ variability in the equatorial Pacific.

L287: clearly delineated? Before you made the argument that is not always so easy? Some peaks are clear, but not all 23.

We have rephrased this sentence.

L293: where is the OMT? Not so much higher sed rates…

We have indicated the OMT in the figure. We have removed the comment wrt higher sed rates across the OMT.

L296-298: what figure do you refer too? (Fig. 5?) Confusing description, the evolutive shows where you see the cycles over the record, maybe state something that the 405 kyr is the most consistently present over the records for all proxies or something of the sort. Also (L298), it is difficult to see the highest amplitudes on the evolutive??? Maybe on the power spectra, but there I don't see a much stronger short eccentricity cycle for the CaCO3, it seems however more present over the whole record, compared to the stable isotope records.

Yes we do refer to figure 5. We have rewritten and clarified this text.

L301-302: indicate on relevant figure(s)where this OMT, and peak glaciation conditions occur

Because we are talking about evolutive analysis, we have removed the reference to glacial peaks. Not all readers are familiar with the structure of the data post-OMT, so this reference was true, but a bit confusing.

L308: 50 kyr cycle, not immediately clear specific for d13C (continuation), or in general. In the d13C tuning this 50 kyr period will be close to 41 kyr, could this be an argument in favour of the d13C tuning (because tuning on the eccentricity makes the obliquity come out stronger, and you would expect an obliquity component no?)???

It is a relatively weak signal indeed. We would like to mention it, but interpreting it is more difficult. We prefer not to use it to favour one age model to the other.

L315-325: it might not be clear to all readers how by looking at Fig. 5 (which shows phases in degrees) you get to duration in kyr, small clarification (e.g. in methodology) would make it easier to interpret. Suggestion.

We have replotted the phase computations and they are now depicted in ky.

L329: Laurin et al., 2017, Paleoceanography, recent reference, maybe include.

We have added this reference.

L332: Is Early Miocene with capital? Indicate your (sub-)stages on your figures.

We prefer informal use. Periods are now indicated on figures.

L343: earlier on you mentioned the variability, sensibility of bandpass filters to varying parameters, now you use the bandpass filters to discuss phase relationships. How robust is this, or is there no problem? Also the phase relationships on Fig. 5 seem to be very sensitive to the used age models…

We have added a cautionary note about the implications of having a short record and not being able to compute this potential phase-increase.

Side question. How is the tuning done? Manually extremum per extremum or with a software/script? Explain somewhere. Suggestion.

We have already explained this in section 4.3.2., last sentence of the second paragraph.

L357: Fig 7e. Peak in sed rate around C6Cn2r, potentially skipping an eccentricity cycle? How would including another short eccentricity cycle in the d13C tuning affect your outcomes?

Probably yes. However, this is the result from an initial 405-ky cycle interpretation in $\delta^{13}C$ and subsequent alignment (in phase) of the ~110-ky cycle. At the OMT this tuning approach results in the (with hindsight incorrect) merging of two cycles into one. Spreading rates rule out this approach, and the in-phase response of $\delta^{13}C$ during (especially) the early Miocene. Including another cycle here, would bring the carbonate and $\delta^{13}C$ tunings in better agreement. However, we would then depart from our phase-assumption. Which is the main cycle parameter we aimed to test.

L358: 1) different units of sedimentation rate in text and figures, confusing. 2) 1.7 cm/kyr peak????

We have adjusted the figure axes to correspond with the text. We have corrected the value of this peak in LSR across the OMT in the text.

L361: could this one cycle difference be related to the comment “L357”?

Yes, it is. We have added this information.

L362: refer again to fig 5, helps with following. (for me)

We have added a reference to Fig. 5.

L368: confusing, different frequencies on fig. 5, and kyr-periods in text descriptions. Would be good to mention the frequencies you point at in the text (or plot evolutive diagrams in function of periods)…
Is the 41 kyr the case for all proxies? See also comment on 50 kyr cycle.

We have added the periodicities to Fig. 5. We have clarified the text with respect to the presence of strong obliquity cycles in benthic $\delta^{18}O$.

L371-379: the phase results for the different proxies seem much more similar to each other than for the CaCO3 tuning. Can you comment on that?

We had noticed this ourselves as well. Unfortunately a small error was present in the phase plots. This has now been corrected.

L385: can refer to the Wilson paper for more info on principle, also on uncertainties etc of this type of data, not all readers might be familiar with this.

We have added a reference to two papers by Wilson.

L393: what are the dotted lines on Fig. 8?

The figure caption is revised to define the dotted lines.

How would this plot look like with the additional d13C short eccentricity in your tuning?

This is not a tuning option considered in this paper. See previous comments.

Side: Why are the sedimentation rate reconstructions for the CaCO3 done on the full eccentricity scale, and for the d13C on a higher resolution???

See the sections related to tuning. $CaCO_3$ is tuned to eccentricity minima. $\delta^{13}C$ to both eccentricity minima and maxima. This is also reflected in the sedimentation rates.

L391-393: conclusions before description results…

We have moved this entire paragraph toward the base of section 5.

L412: reference to Tab. 1 would be useful. In the text you use duration difference, which are not includes in the Table… could make it easier for the reader.

We have added this reference.

L426-427: specify which interval.

We have specified this.

L435: On=> One? Typo.

We have rephrased this sentence to clarify the main message.

L443: I expected this discussion much earlier… it affects the interpretation of the previous paragraphs

We prefer the order in which we presented the results and discussion. First we present two tunings. Next we let spreading rates be the judge. Finally, we integrate all results (tuning and spreading rates) and explain the key differences between the two tuned age models.

L468: be consistent in ref style.

Corrected.

L494: Zachos et al. (2010), EPSL interesting additional reference?…

This is a reference regarding the PETM and early Eocene. Carbon cycle dynamics were probably quite different then.

L501: Laurin et al., 2017; Paleoceanography.

We have added Laurin et al to the references here.

L503-505: where do we see this change???

We have added this information between parentheses.

Fig 6 & 7: detrended records? Mention.

Records are not detrended in the plots, but were detrended prior to filtering. This is mentioned in the methods section.

L509-510: What might be the influence of the detrending (or not fully) of this d13C shift? Might it effect the BP filtering, be related to this peak in SR in C6Cn2r, add in the end an offset in age models??? Just an observation/thought…

We have tested the affect of detrending, but this did not affect the BP filtering of the 405 ky or the ~110-kyr signal significantly.

L519: the CacO3 content in this case is a 'derivative' of original MS data…

We have added this information.

L525: 'insolation forcing' (actually also in your discussion), you tune on eccentricity, but eccentricity as such is only a very small component in the insolation term, eccentricity kicks in as amplitude modulator, non-linear feedbacks etc… should we be careful with the terminology?

We have rephrased this.

L533: "C6AAr.r3" = only place in the manuscript where this name occurs???? Typo? Different notation, then explain.

This was indeed an error. We have corrected it.

We would like to thank R2 for their constructive comments.

Astronomical tunings of the Oligocene-Miocene Transition from Pacific Ocean Site U1334 and implications for the carbon cycle

Helen M. Beddow[1], Diederik Liebrand[2, 3, *], Douglas S. Wilson[4], Frits J. Hilgen[1], Appy Sluijs[1], Bridget S. Wade[5], Lucas J. Lourens[1]

[1]Department of Earth Sciences, Faculty of Geosciences, Utrecht University, Utrecht, The Netherlands; [2]PalaeoClimate.Science, Utrecht (province), The Netherlands [3]MARUM - Center for Marine Environmental Science, University of Bremen, Bremen, Germany; [4]Department of Earth Science University of California, Santa Barbara (CA), United States; [5]Department of Earth Sciences, Faculty of Mathematical and Physical Sciences, University College London, Gower Street, London, United Kingdom; [*]Corresponding author: diederik@palaeoclimate.science

Abstract

Astronomical tuning of sediment sequences requires both unambiguous cycle-pattern recognition in climate proxy records and astronomical solutions, and independent information about the phase relationship between these two. Here we present two different astronomically tuned age models for the Oligocene-Miocene Transition (OMT) from Integrated Ocean Drilling Program Site U1334 (equatorial Pacific Ocean) to assess the effect tuning has on astronomically calibrated ages and the geologic time scale. These alternative age models (roughly from ~22 to ~24 Ma) are based on different tunings between proxy

records and eccentricity: the first age model is based on an aligning $CaCO_3$ weight (wt%) to Earth's orbital eccentricity, the second age model is based on a direct age calibration of benthic foraminiferal stable carbon isotope ratios ($\delta^{13}C$) to eccentricity. To independently test which tuned age model and associated tuning assumptions is in best agreement with independent ages based on tectonic plate-pair spreading rates, we assign the tuned ages to magnetostratigraphic reversals identified in deep-marine magnetic anomaly profiles. Subsequently, we compute tectonic plate-pair spreading rates based on the tuned ages. The resultant, alternative spreading rate histories indicate that the $CaCO_3$ tuned age model is most consistent with a conservative assumption of constant, or linearly changing, spreading rates. The $CaCO_3$ tuned age model thus provides robust ages and durations for polarity chrons C6Bn.1n–C7n.1r, which are not based on astronomical tuning in the latest iteration of the Geologic Time Scale. Furthermore, it provides independent evidence that the relatively large (several 10,000 years) time lags documented in the benthic foraminiferal isotope records relative to orbital eccentricity, constitute a real feature of the Oligocene-Miocene climate system and carbon cycle. The age constraints from Site U1334 thus provide independent evidence that the delayed responses of the Oligocene-Miocene climate-cryosphere system and (marine) carbon cycle resulted from highly nonlinear feedbacks to astronomical forcing.

Keywords

Astronomical tuning, marine carbon cycle, Oligocene Miocene Transition, IODP Site U1334, equatorial Pacific Ocean, geologic time scale

1. Introduction

Astronomically tuned age models are important in studies of Cenozoic climate change, because they shed light on cause and effect relationships between insolation forcing and the linear and nonlinear responses of Earth's climate system (e.g., [*Hilgen et al*., 2012, *Vandenberghe et al.*, 2012; *Westerhold et al.,* 2017]). As more Cenozoic paleoclimate records are generated that use astronomical tuning as the main high-precision dating tool, it is important to understand the assumptions and limitations inherent in this age-calibration method, in particular with respect to assumptions related to phase-relationships between tuning signal and target curves (i.e., climate proxy records and astronomical solutions, respectively). These phase assumptions have implications for (*i*) determining the absolute timing of events, (*ii*) the understanding of leads and lags in the climate system, and (*iii*) the exact astronomical frequencies that are present in climate proxy records after tuning.

Previously published astronomically tuned age-models for high-resolution climate records that span the Oligocene-Miocene Transition (OMT, ~23 Ma), have used different tuning signal curves for sites from different paleoceanographic settings. In addition, different tuning target curves have been applied. For example, records from Ocean Drilling Program (ODP) Sites 926 and 929 from the Ceara Rise (equatorial Atlantic) were tuned using magnetic susceptibility and/or color reflectance records (i.e., proxies for bulk sediment carbonate content) as tuning signal curve, and used obliquity as the main tuning target curve, sometimes with weaker precession and eccentricity components added (e.g. [*Pälike et al.*, 2006a; *Shackleton et al.*, 1999, 2000; *Zachos et al.*, 2001]). In contrast, sediments from ODP Site 1090 from the Agulhas Ridge (Atlantic sector of the Southern Ocean) and ODP Site 1218 from the

equatorial Pacific Ocean were tuned using benthic foraminiferal stable oxygen ($\delta^{18}O$) and/or carbon ($\delta^{13}C$) isotope records as tuning signal (e.g. [*Billups et al.*, 2004; *Pälike et al.*, 2006b]). These records used different combinations of eccentricity, obliquity and/or precession as tuning targets (ETP curves).

More recently, Oligocene-Miocene records from ODP Site 1264 and Middle Miocene records from Integrated Ocean Drilling Program (IODP) Site U1335 used the Earth's eccentricity solution as the sole tuning target. These studies used lithological data, such as elemental estimates based on X-ray fluorescence (XRF) core scanning records, as the sole tuning signal. The records from both these sites are characterized by a clear expression of eccentricity, either resulting from productivity dominated cycles (at Site 1264, [*Liebrand et al.*, 2016]) or dissolution dominated cycles (at Site U1335, [*Kochhann et al.*, 2016]). The general phase relationships between the ~110-ky cycles and 405-ky cycles (in case of Site U1335), in lithologic records and the stable eccentricity solution for this interval [*Laskar et al.*, 2010, *Laskar et al.*, 2011], i.e., whether maxima in signal-curve correspond to minima or maxima in target-curve, were straightforward to derive [*Liebrand et al*, 2016, *Kochhann et al.*, 2016]. These broad scale phase relationships were in agreement with those previously derived using benthic foraminiferal $\delta^{18}O$ and $\delta^{13}C$ records (e.g., [*Zachos et al*, 2001, *Pälike et al*, 2006b]).

The different options for astronomical age calibration of the Oligocene-Miocene time interval has resulted in large variations in the precise phase-estimates after tuning between ~110-ky and 405-ky cycles present in both the eccentricity solution and in lithologic and climatologic proxy records. In addition, the choice of tuning signal

curve may result in different cyclostratigraphic interpretations, and different ages and durations of geologic events. To obtain better constraints for the true phase-relationships of the ~110-ky and 405-ky cycles between benthic foraminiferal stable isotope records and orbital eccentricity, and to better understand the implications that initial phase-assumptions for astronomical age calibration have on absolute ages across the OMT, we need independent dates that are free from tuning phase-assumptions. Previous studies have successfully used plate-pair spreading rates to date magnetochron reversals and used these ages as independent age control (e.g., [*Hilgen et al.*, 1991, *Lourens et al.*, 2004]).

Here, we present two astronomically tuned age models for newly presented (estimates of) sediment $CaCO_3$ content and previously published high-resolution benthic foraminiferal $\delta^{18}O$ and $\delta^{13}C$ records across the OMT from IODP Site U1334 (eastern equatorial Pacific Ocean) [*Beddow et al.,* 2016]. We select the sediment $CaCO_3$ content and benthic foraminiferal $\delta^{13}C$ as tuning signals, because these data are generally thought represent two end-members in terms of tuning phase assumptions [*Pälike et al.*, 2006, *Liebrand et al.*, 2016]. We evaluate the ramifications of using these different tuning proxies for (*i*) absolute ages of magnetochron reversals, and (*ii*) the leads and lags between eccentricity tuning target and lithologic/paleoclimate tuning signals. We achieve this, by computing the spreading rate histories of a suite of tectonic plate-pairs, after assigning the astronomically tuned ages to the magnetostratigraphic reversals in their anomaly profiles. The constraints given by the long-term evolutions of these alternative spreading-rate histories are sufficiently precise to discriminate between tuning options and phase assumptions.

2. Materials and Methods

2.1 Site description

Site U1334, located in the eastern equatorial Pacific (4794 meters below sea level (mbsl), 7°59.998′N, 131°58.408′W), was recovered during IODP Expedition 320 (Fig. 1). Upper Oligocene and lower Miocene sediments from Site U1334 were deposited at a paleodepth of ~4200 mbsl and consist of foraminifer- and radiolaria-bearing nannofossil ooze and chalk [*Pälike et al.*, 2010, 2012]. An expanded Oligocene-Miocene section with a well-defined magnetostratigraphy was recovered [*Pälike et al.*, 2010; *Channell et al.*, 2013], and a continuous spliced record of Holes A, B and C was placed on a core composite depth scale below seafloor (CCSF-A, equivalent to meters composite depth; Figs. 2 and 3) [*Westerhold et al.*, 2012a]. Samples were taken along the splice and all results presented here follow this depth model [*Beddow et al.*, 2016].

2.2 Coulometric $CaCO_3$ and magnetic susceptibility

Lithological records from Site U1334 that span the OMT show large variability in $CaCO_3$ content [*Pälike et al.*, 2010]. To obtain a high-resolution and continuous lithological proxy record, we estimate $CaCO_3$ wt% of the dry sediment (hereafter: $CaCO_3$ content), by calibrating high-resolution shipboard magnetic susceptibility data (MS) to lower resolution discrete shipboard coulometric $CaCO_3$ measurements for Site U1334 [*Pälike et al.*, 2010]. Minimum MS values correspond to maximum $CaCO_3$ values. The correlation between coulometric $CaCO_3$ measurements and MS was calculated using a linear regression line, with an R^2 value of 0.92 (Fig. 2), indicating that ~90% of the variability in the MS record is caused by changes in the bulk sediment $CaCO_3$ content. Middle Miocene $CaCO_3$ records from nearby Site

U1335 show negatively skewed cycle shapes and have been interpreted as a dissolution-dominated signal [*Herbert*, 1994, *Kochhann et al*., 2016]. In contrast, cycle shapes in the $CaCO_3$ content record for the Oligocene-Miocene of Site U1334 are less skewed, suggesting that here $CaCO_3$ content was predominantly controlled by a combination of productivity and dissolution.

2.3 Benthic foraminiferal stable isotope records and magnetostratigraphic age model

We use the benthic foraminiferal $\delta^{18}O$ and $\delta^{13}C$ records of Site U1334, which were measured on the *Oridorsalis umbonatus* and *Cibicidoides mundulus* benthic foraminifer species [*Beddow et al*., 2016]. To construct this mixed-species record, *O. umbonatus* values were corrected to *C. mundulus* values based on ordinary least squares linear regression that was based on the analysis of 180 pairs of for inter-species isotope value comparison was applied (for details see [*Beddow et al*., 2016]). The benthic foraminiferal stable isotope datasets at Site U1334 were placed on a magnetostratigraphic age model calculated by fitting a third-order polynomial through 14 magnetostratigraphic age-depth tie-points. Twelve of these chron boundaries fall within the study interval, are given in Table 1, and are shown in Figs. 3 and 4. This magnetostratigraphic age model yields an initial duration of ~21.9 to 24.1 Ma for the study interval (Fig. 4) [*Channell et al*., 2013; *Beddow et al.,* 2016].

2.4 Spectral analysis

We use the statistical software program AnalySeries [*Paillard et al*., 1996] to conduct spectral analyses on the benthic foraminiferal $\delta^{13}C$ and $\delta^{18}O$ and the $CaCO_3$ datasets in the depth domain, on the magnetostratigraphic age model [*Beddow et al*., 2016],

and on both astronomically tuned age model options presented here. Prior to analysis, the $CaCO_3$ content and stable isotope data were re-sampled at 2 and 5 cm in the depth domain, and at 2.5 and 3.0 ky in the age domain, respectively, and trends longer than 6 m, or 600 ky, were removed using a notch-filter [*Paillard et al.*, 1996]. Blackman Tukey spectral analysis was used to identify dominant periodicities present within the data, which subsequently were filtered using Gaussian filters. We applied cross-spectral analysis to identify coherency and phase relationships between the eccentricity and the $CaCO_3$, $\delta^{18}O$ and $\delta^{13}C$ chronologies. These calculations were performed at 95% significance. Evolutive spectral analyses, using a sliding Fast Fourier Transform (FFT), were computed using MATLAB.

2.5. Reversal ages based on plate-pair spreading rates

We use previously published magnetic anomaly profiles of tectonic plate pair spreading rates [*Wilson*, 1993] to independently test the astronomical age models for Site U1334. This age comparison method is similar to that previously used to support astronomically tuned age models for the Miocene, Pliocene and Pleistocene [*Hilgen et al.*, 1991; *Krijgsman et al.*, 1999; *Hüsing et al.*, 2007]. We have selected plate pairs with high quality anomaly profiles and relatively high spreading rates. These plate-pairs are in order of decreasing spreading rate: Pacific-Nazca, Pacific-Juan de Fuca, Australia-Antarctic, and Pacific-Antarctic. Data for the Pacific-Nazca pair is limited to the northern part of the system, which is well surveyed from studies of the separation of the Cocos plate from the northern Nazca plate during chron C6Bn [*Lonsdale*, 2005; *Barckhausen et al.,* 2008]. Pacific-Juan de Fuca data are from immediately north of the Mendocino fracture zone. Reversal ages based on these spreading rates are also used in previous timescale calibrations [e.g. *Cande and Kent*,

1992] despite the fact that for the Oligocene-Miocene time interval only the Pacific-plate record has survived and the Juan de Fuca plate was subducted. *Wilson* [1988] interpreted a sudden change of spreading-rate gradient for this pair from south faster prior to C6Cn.2n(o) to north faster after that reversal. The dataset for the Australia-Antarctic pair is similar to that presented by *Cande and Stock* [2004]. It is expanded from that used by *Lourens et al.* [2004] who assigned reversal ages spanning from 18.524 Ma to 23.030 Ma for the chron interval from C5Er (top) to C6Cn.2n (base), based on a linear interpolation of spreading rates of 69.9 mm/yr for this plate pair. Data for Pacific-Antarctic come primarily from more recent surveys near the Menard and Vacquier fracture zones [*Croon et al*., 2008].

3. Results

3.1. Lithologic and paleoclimatic records

The synthetic wt% calcium carbonate record ($CaCO_3$ content wt%) ranges between ~45% and 95%, consistent with the coulometric $CaCO_3$ wt% measurements on discrete samples (Figs. 2, 3). Variability is generally twice as large in the lower Miocene section of the record, between 88.95 and ~102 m CCSF-A (core composite depth below sea floor), varying by ~40% with several minima in the record dipping below 70% (Fig. 3). There is little variability in $CaCO_3$ content, across the OMT, between ~102 and ~106 m CCSF-A. The benthic foraminiferal $\delta^{18}O$ record captures a large, partially transient, shift towards more positive values at the Oligocene-Miocene boundary, with maximum values of ~2.4 ‰ occurring at 104.5 CCSF-A (Fig. 2). After the boundary, both $\delta^{18}O$ and $\delta^{13}C$ values show higher amplitude variability, and more permanent shifts towards higher values [*Beddow et al*., 2016].

3.2. Spectral Analysis in the depth domain

The power spectra of the $CaCO_3$ content record in the depth domain reveal strong spectral peaks at frequencies of 0.20 cycles/m and 0.65 cycles/m (Fig. 3). These frequencies broadly correspond to those found in the benthic foraminferal $\delta^{18}O$ and $\delta^{13}C$ depth series at 0.15 cycles/m and 0.65 cycles/m [*Beddow et al.*, 2016]. High-amplitude cycles with frequencies in the range between ~0.20 and 0.80 cycles/m are present in all datasets with an approximate 1:4 ratio, suggesting a strong influence of eccentricity on the records (i.e. ~110:405 ky cycles). This interpretation of strong eccentricity is supported by the application of the initial magnetostratigraphic age model [*Beddow et al.*, 2016].

4. Astronomical tunings of Site U1334

4.1 Initial age model

As a starting point for astronomical tuning we use an initial magnetostratigraphic age model [*Beddow et al*, 2016; *Channel et al.*, 2013], which is based on the chron reversal ages of the 2012 Geologic Time Scale (GTS2012, [*Vandenberghe et al.*, 2012; *Hilgen et al.*, 2012], see Table 1, Fig. 4.). On this initial age model, (time-evolutive) power spectra demonstrate that the $CaCO_3$ content and benthic foraminiferal $\delta^{18}O$ and $\delta^{13}C$ records are dominated by ~110 ky and 405 ky eccentricity paced cycles, with short intervals of strong responses at higher frequencies (Fig. 5). To further assess the influence of eccentricity on the records from Site U1334, we filter the ~110-ky and 405-ky cycles of the $CaCO_3$ content and $\delta^{13}C$ records (Figs. 6a and 7a). In total, we observe just over five 405-ky cycles in both the filtered $CaCO_3$ content and $\delta^{13}C$ records. There is a notable difference in the number of filtered ~110-ky cycles present between these two datasets. We observe

250 twenty-three ~110-ky cycles in the $CaCO_3$ content record, and twenty-one in the $\delta^{13}C$
251 record. Visual assessment of the number of cycles is not always straightforward,
252 because not every ~110-ky cycle is expressed equally strong in all data records. In the
253 eccentricity solution for the interval approximately between 21.9 and 24.1 Ma, we
254 count five and a half 405-ky cycles and twenty-two ~110-ky cycles. These numbers
255 are largely in agreement with those obtained from visual assessment and Gaussian
256 filtering.
257
258 **4.2 Astronomical target curve**
259 For our astronomical target curve, we select Earth's orbital eccentricity. Timeseries
260 analyses on the $CaCO_3$ content, and the benthic foraminiferal $\delta^{18}O$ and $\delta^{13}C$ records
261 in the depth domain, and on the initial age model, indicate that eccentricity is the
262 dominant cycle and that higher-frequency cycles are intermittently expressed (Fig. 5).
263 Additional reasons to select eccentricity as the sole tuning target for the OMT of Site
264 U1334 are the uncertain phase relationships of the data records to precession, and the
265 unknown evolution of tidal dissipation and dynamical ellipticity before 10 Ma
266 [*Zeeden et al*., 2014]. These parameters affect the long-term stability of both the
267 precession and obliquity solutions [*Lourens et al.,* 2004*; Husing et al.,* 2007]. We use
268 the most recent nominal eccentricity solution (i.e., La2011_ecc3L) [*Laskar et al.,*
269 2011a, 2001b; *Westerhold et al*., 2012b] as tuning target, and for the OMT interval
270 this solution is not significantly different from the La2004 eccentricity solution
271 [*Laskar et al.*, 2004], which was used to generate previous astronomically tuned high-
272 resolution age models for this time interval [*Pälike et al.*, 2006a,b].
273
274 **4.3. Astronomical age calibration of the OMT from Site U1334**

To test different ages and durations of the data from Site U1334, and the leads and lags of climate cycles with respect to eccentricity, we first consider the $CaCO_3$ content record and then the benthic foraminiferal $\delta^{13}C$ record as tuning signals. Both tuning options are underpinned by assumptions of a consistent and linear in-phase relationship between the tuning signal and the eccentricity target. Previously tuned climate records for the OMT have shown that these two datasets represent end-members with respect to phase assumptions, with $CaCO_3$ content showing no lag or the smallest lag with respect to orbital eccentricity, and $\delta^{18}O$ and $\delta^{13}C$ showing increasingly larger lags to the ~110-ky and 405-ky eccentricity cycles [*Liebrand et al.*, 2016, *Pälike et al.*, 2006a, *Pälike et al.*, 2006b]. Thus, by selecting the $CaCO_3$ content record and the benthic foraminiferal $\delta^{13}C$ chronology, we span the full range of tuned ages that different phase-assumptions between eccentricity and proxy data possibly could imply. We expect that the $CaCO_3$ tuned age model is in best agreement with independent ages based on spreading rates, and hence, that benthic foraminiferal $\delta^{13}C$ will show the largest lag with respect to eccentricity.

4.3.1. Astronomical tuning using the $CaCO_3$ content record

We use the initial magnetostratigraphic age model as a starting point for a more detailed ~110-ky calibration of $CaCO_3$ content of the sediment to eccentricity. $CaCO_3$ maxima, mainly reflecting increased surface ocean productivity and/or decreased deep-ocean dissolution [e.g. *Hodell et al.*, 2001], generally correspond to more positive $\delta^{18}O$ values, which are indicative of cooler, glacial periods. Hence, both bulk $CaCO_3$ content and benthic foraminiferal $\delta^{18}O$ values are linked to eccentricity minima and are therefore anticorrelated with eccentricity [*Zachos et al.*, 2001; *Pälike et al.*, 2006a; *Pälike et al.*, 2006b]. The $CaCO_3$ content record is characterized by

strong maxima, which we manually aligned to ~110-ky eccentricity minima by visually selecting tie-points (Fig. 6c). In addition to these well expressed ~110-ky cycles, we take the expression of the 405-ky cycle into account to establish the tuned age model. The data records from Site U1334 span the interval between 21.96 and 24.15 Ma (2.19 My duration) on the $CaCO_3$ tuned age model. Linear sedimentation rates (LRS) vary between 0.9 and 2.2 cm/ky (Fig. 6). On average this yields a sample resolution of 3.6 ky for the benthic foraminiferal isotope records.

Evolutive analyses (i.e., FFT using a sliding window) of the $CaCO_3$ content and benthic foraminiferal $\delta^{18}O$ and $\delta^{13}C$ records on the $CaCO_3$ tuned age model indicate that the 405-ky cycle is relatively strongly expressed in all datasets (Fig. 5). However, this signal is weaker or absent across the OMT (~23 Ma) in the evolutive spectrum of $CaCO_3$ content, and post-OMT in benthic foraminiferal $\delta^{18}O$. The ~110-ky cycle is present in the data records on the $CaCO_3$ tuned age model between 23.4 and 22.2 Ma for $CaCO_3$ content, between 23.0 and 22.2 for benthic foraminiferal $\delta^{18}O$, and between 22.8 and 22.2 in benthic foraminiferal $\delta^{13}C$. The ~110-ky cycle is particularly pronounced in in both the $CaCO_3$ and the benthic foraminiferal $\delta^{18}O$ records, and we can identify power at both the 125 ky and the 95 ky eccentricity cycles. We note that this could be a direct result from using eccentricity as a tuning target (see e.g., [*Shackleton et al.*, 1995; *Huybers and Aharonson*, 2010). For $\delta^{13}C$, the evolutive analysis and power spectra indicate that ~110 ky cycle is more strongly expressed at the 125-ky periodicity, compared to the 95-ky component. We find intermittent power present at a periodicity of ~50 ky/cycle, which is either related to the obliquity cycle that is offset towards a slightly longer periodicity, or to the first harmonic of the ~110-ky eccentricity cycle [*King*, 1996]. The ~50-ky cycle is best

expressed in the benthic foraminiferal $\delta^{18}O$ record on the $CaCO_3$ tuned age model, where we identify two main intervals with significant power at this periodicity, one between ~23.5 and ~23.8 Ma, and the other between ~22.4 and ~22.6 Ma (Fig. 5).

Cross-spectral analyses between the $CaCO_3$ content, $\delta^{18}O$ and $\delta^{13}C$ records on the $CaCO_3$ tuned age model and eccentricity, indicate that all are significantly coherent at the 405-ky, 125-ky and 95-ky eccentricity cycles (Fig. 5). Phase estimates of benthic foraminiferal $\delta^{18}O$ with respect to eccentricity indicates a lag of 21±16 ky at the 405 ky period, and 9±3 ky at the ~110 ky periodicity (95% confidence on error bars). The $\delta^{13}C$ record lags eccentricity by 29±14 ky at the 405-ky cycle, by 9±4 ky at the ~110-ky cycle (Fig. 5). The coherence between $CaCO_3$ content and eccentricity is only just significant, and phase estimates roughly in-phase with eccentricity; 6±24 ky at the 405 ky cycle, and −1±2 ky at the ~110-ky cycle. These phase estimates between $CaCO_3$ content and eccentricity are not surprising, because $CaCO_3$ content was used to obtain astronomically tuned ages. These phase relationships between $CaCO_3$ and eccentricity thus confirm that the in-phase tuning assumption was applied successfully.

4.3.2. Astronomical tuning using the benthic foraminiferal $\delta^{13}C$ record

An important consequence of the $CaCO_3$ tuned age model is that eccentricity-related variability within the benthic foraminiferal $\delta^{13}C$ record is not in-phase with eccentricity (Fig. 7b; [*Laurin et al.*, 2017]). On both the initial magnetostratigraphic age model and on the $CaCO_3$ tuned age model, the phase-lag, as visually identified in the filtered records, between the 405-ky-eccentricity cycle and the 405-ky cycle in $\delta^{13}C$ increases during the early Miocene (Figs. 6 and 7). The 405-ky eccentricity

pacing of $\delta^{13}C$ is a consistent feature that characterizes the Cenozoic carbon cycle [*Holbourn et al*., 2004, 2013; *Littler et al*., 2014; *Pälike et al*., 2006a,b; *Liebrand et al*., 2016], and to date no large changes in phase-relationship have been documented. However, the increased phase lag in the response of the 405-ky cycle in $\delta^{13}C$ to eccentricity, as is suggested by the $CaCO_3$ tuned age model, could provide further support for a large-scale reorganization of the carbon cycle across the OMT as has previously been suggested based on a sudden increase in accumulation rates of benthic foraminifera and Uranium/Calcium values, suggesting increased organic carbon burial [*Diester-Haas et al*., 2011, *Mawbey and Lear*, 2013].

To test the validity of the large phase-lag of the 405-ky cycle in benthic foraminiferal $\delta^{13}C$ to eccentricity, and to test the potential increase of this lag, we generate another astronomically tuned age model. This time, we use the benthic foraminiferal $\delta^{13}C$ record as the tuning signal and assume that the 405-ky cycles and ~110-ky cycles in benthic foraminiferal $\delta^{13}C$ are in-phase with eccentricity across the OMT (Fig. 7d). Approximately five 405-ky cycles are identified in the benthic foraminiferal $\delta^{13}C$ record, which facilitate initial visual alignment to the same cycle in the eccentricity solution. Subsequently, we correlated the maxima and minima in the of the benthic foraminiferal $\delta^{13}C$ record, as identified in Gaussian filters centered around the ~110-ky cycle of this record on the initial magnetostratigraphic age model (Fig. 7a), to those identified in the filtered component of the eccentricity solution (Fig. 7d).

The data records, on the benthic foraminiferal $\delta^{13}C$ tuned age model, span the interval between 22.1 and 24.2 Ma (i.e., 2.1 My duration), resulting in an average time step of 3.4 ky for the benthic stable isotope records. LRS generally range between 0.7 and 2.5

cm/ky, apart from an abrupt and short-lived increase across the OMT to ~3.3 cm/ky. On the $\delta^{13}C$ tuned age model, the $CaCO_3$ record remains in anti-phase with respect to ~110-ky eccentricity, but the benthic foraminiferal $\delta^{13}C$ tuning results in an alternative alignment $CaCO_3$ cycles to eccentricity, yields a ~110-ky shorter duration of the data records, and causes the sudden increase in sedimentation rates across the OMT (Fig. 6 and 7). The evolutive analyses and power spectra are broadly consistent with the evolutive analyses from the $CaCO_3$ tuned age model, with dominant 405-ky cyclicity in all three datasets, an increase in spectral power at ~110-ky eccentricity cycles after the OMT and intermittent expression of higher frequency astronomical cycles (Fig. 5). On the $\delta^{13}C$ tuned age model, all datasets exhibit a relatively stronger response at the 95-ky short eccentricity cycle than the 125-ky short eccentricity cycle, in contrast to the $CaCO_3$ tuned age model. In the late Oligocene, between ~ 23.3 and 23.8 Ma, strong 40-ky obliquity cycles are present in the benthic foraminiferal $\delta^{18}O$ record on the $\delta^{13}C$ tuned age model.

Cross-spectral analyses between the $CaCO_3$ content, $\delta^{18}O$ and $\delta^{13}C$ records on the $\delta^{13}C$ tuned age model and eccentricity, indicate that all are significantly coherent at the 405-, 125- and 95-ky eccentricity cycles (Fig. 5). $CaCO_3$ content leads eccentricity by −24±18 ky at the 405-ky cycle, by −7±3 ky at the ~110-ky cycle. On the $\delta^{13}C$ tuned age model, phase estimates of $\delta^{18}O$ with respect to eccentricity shows small leads of −4±12 ky at the 405-ky cycle, and of −1±4 ky at the ~110-ky cycle. Benthic foraminiferal $\delta^{13}C$ lags eccentricity by 19±8 ky at the 405-ky cycle and by 3±2 ky at the ~110-ky eccentricity cycle, which is congruent with the in-phase tuning assumption between benthic foraminiferal $\delta^{13}C$ and eccentricity that is used in this age model.

4.3.3. Age model comparison

The final eccentricity tuned age models for the OMT time interval differ for two reasons. Firstly, there are 21 complete 110 ky cycles in the $\delta^{13}C$ tuned age model, and 22 in the $CaCO_3$ content record. The tuned age models are largely consistent with each during the late Oligocene and OMT interval. The base of Chron C6Cn.2n, which marks the Oligocene-Miocene boundary, occurs within 10 ky on both age models. The two astronomically tuned age models diverge at ~22.7 Ma, where the $CaCO_3$ content has an additional ~110 ky cycle on the initial magnetostratigraphic age model. A second factor contributing to the difference between the two astronomically tuned age models is the different phase relationships between the two proxy records and eccentricity (i.e., either $CaCO_3$ is in-phase eccentricity, or benthic foraminiferal $\delta^{13}C$). These different phase assumption that underpin the two tuned age models account for age differences up to 10% at all periodicities in the two records (Table 2), in addition to the ~110-ky difference for the early Miocene interval of Site U1334 that results from the two different cyclostratigraphic interpretations. In turn, these interpretations are resultant from the initial phase-assumptions. The longer lag time of $\delta^{13}C$ with respect to eccentricity, in comparison with $CaCO_3$, leads to older ages assigned to ~110 kyr cycles in the $\delta^{13}C$ age model. This is particularly notable between 22.7 Ma and 24.2 Ma, when the difference between the age models is accounted for only by the difference in phase.

5. Spreading rates

To independently test whether the $CaCO_3$ tuned ages or the benthic foraminiferal $\delta^{13}C$ tuned ages and their underlying phase-assumption, are most appropriate for tuning the

deep marine Oligocene-Miocene records from Site U1334, we assign the tuned magnetostratigraphic reversal ages from Site U1334 to those identified in anomaly profile of tectonic plate pairs. We use the evolution through time of the spreading rates of these plate pairs as a control for our tuned age models [*Wilson*, 1993; *Krijgsman et al*., 1999]. Rapid simultaneous fluctuations in the spreading rate of multiple plate pairs are highly unlikely and indicate errors in the tuned timescale. We propose to use the astronomically tuned age model from Site U1334 that passes this test most successfully to provide ages for C6Bn.1n (o) to C7n.1r (o) and potentially revise those currently presented in the GTS2012.

On the $CaCO_3$ tuned age model, the Australia-Antarctica, Pacific-Nazca, and Pacific-Antarctic plate pairs are all very close to a constant spreading rate (Fig. 8). The Juan de Fuca-Pacific plate-pair indicates a sudden decrease in spreading rate (145 to 105 mm/yr) at ~23 Ma, consistent with expectations (see the above section **2.5**; [*Wilson*, 1988]). In contrast, the synchronous changes for the Australia-Antarctica, Pacific-Nazca, and Pacific-Antarctic plate pairs in the $\delta^{13}C$ tuned age model, especially the faster spreading rates ~22.5-23.0 Ma implied by older ages for C6Bn, make this tuning option less plausible. Differences between the $CaCO_3$ tuned age model for Site U1334 and GTS2012 are subtler. The longer duration of C6Cn.3n in the $CaCO_3$ tuned age model (106 vs. 62 kyr, Table 1) eliminates a brief, and relatively small, pulse of fast spreading implied by GTS2012, visible in Figure 8a as positive slopes in age-distance during that chron. Over longer intervals, $CaCO_3$ tuned ages remove a slight but synchronous rate slowdown that is also implied by GTS2012 and which starts at ~23.2 Ma.

The $CaCO_3$ tuned age model indicates a duration for C6Cn.2n of 67 ky. This duration may be up to ~40 ky too short, as is suggested by the relatively short-lasting increase in spreading rates during this chron (see the positive slopes in Figure 8b). The spreading-distance error bars indicate that this age discrepancy is marginally significant, with no overlap in reduced distance for the boundaries of this chron for three of four plate pairs. Despite this small uncertainty in the duration for chron C6Cn.2n on the $CaCO_3$ tuned age model, the base of this chron appears in good agreement with spreading rates and thus suggests a slightly older age for the Oligocene-Miocene boundary of approximately 23.06 Ma. Furthermore, the polarity chron ages from the $CaCO_3$ tuned ages are generally older by approximately 40 ky on average than those presented in the GTS2012 (Table 1). In both the $CaCO_3$ content and $\delta^{13}C$ record, the short interval around C6Cn.2n is difficult to align to the eccentricity solution (Figs. 5 and 6), because $CaCO_3$ content values are high, with little variability and benthic foraminiferal $\delta^{13}C$ values corresponds to the marked shift towards higher values at the Oligocene-Miocene carbon maximum [*Hodell and Woodruff*, 1994]. The 83 kyr duration of C6Cn.2n from the $\delta^{13}C$ tuned age model is better supported by spreading rates than the 67 kyr duration from the $CaCO_3$ tuned age model, and the 118 kyr duration in GTS2012 is even more consistent with constant spreading rates. If we extrapolate constant spreading rates across C6Cn.2n, using the $CaCO_3$ tuned age for the base of 23.06 Ma, we obtain an age for the top of this normal polarity interval of ~22.95 Ma, and a duration of 110 ky. An important implication of the $CaCO_3$ tuned ages is the delayed increase in spreading rates of the Juan de Fuca-Pacific plate-pair. On the $CaCO_3$ tuned age model this occurred approximately 200 ky later than those ages presented in the GTS2012 (i.e. during Chron C6Cn.2n. instead of C6Cn.3n, respectively; see Fig 8).

6. Discussion

6.1. Evaluation of tuning signals

Of the two astronomically tuned age models and GTS2012, the $CaCO_3$ tuned age model is most consistent with the assumption of the least amount of changes in plate-pair spreading rates, which makes it the preferred astronomically tuned age model option for Site U1334. (Fig. 8). This agreement between plate pair spreading rate history and the $CaCO_3$ tuned ages, suggests that local/regional (i.e., lithological) tuning signals can produce more accurate age models in comparison with age models based on globally integrated isotope records. The latter data are known to produce significant lags relative to eccentricity as a result of highly nonlinear feedback mechanisms [*Laurin et al.*, 2017; *Pälike et al.*, 2006b; *Zeebe et al.*, 2017]; a result that is confirmed by this study (Table 2). The independent evidence that we provide for using a lithological (proxy) record for astronomical age calibration of marine sediments yields further support for similar astronomical tuning methods. Examples are: the Middle Miocene [*Kochhann et al.*, 2016] and Eocene-Oligocene [*Westerhold et al.*, 2015] records from the equatorial Pacific Ocean, and the Oligocene-Miocene records from the South Atlantic Ocean [*Liebrand et al.*, 2016]. We note, however, that these records show variable ratios of productivity to dissolution as the main source of variance in the data. Future, additional testing of phase-uncertainties could include statistical approaches, such as Monte Carlo simulations [*Khider et al.*, 2017].

6.2 Implications for the carbon cycle

Benthic foraminiferal $\delta^{13}C$ variations in the open ocean are typically interpreted to reflect the ratio between global organic and inorganic carbon burial [*Shackleton*,

1977; *Broecker*, 1982; *Diester-Haas et al.*, 2013, *Mawbey and Lear*, 2013].

Astronomical forcing of organic carbon burial is typically expected in the precessional band because organic carbon burial, notably in the marine realm, depends on clay fluxes and thus hydrology [*Berner et al.*, 1983]. However, the residence time of carbon (~100 kyr) is so long [*Broecker and Peng*, 1982] that this energy is transferred into eccentricity bands [*Pälike et al.*, 2006; *Ma et al.*, 2011; *Laurin et al.*, 2017]. Importantly, while the total marine carbon inventory is driven by ocean chemistry, the phase lag between eccentricity forcing and $\delta^{13}C$ should primarily be a function of the residence time of carbon [*Zeebe et al.*, 2017]. Hypothetically, a change in total organic matter burial will only result in whole-ocean steady state when the $\delta^{13}C$ of buried carbon equals that of the input (through rivers). Because the burial fluxes are small compared to the total carbon inventory, a pronounced time lag between eccentricity forcing and $\delta^{13}C$ is expected [e.g., *Zeebe et al.*, 2017].

Interestingly, the $CaCO_3$ age model for Site U1334 suggests that the phase lag between the 405 ky cycle in the $\delta^{13}C$ record and the eccentricity forcing increases across the OMT (see position of minima and maxima of the 405 ky filters of eccentricity and benthic foraminiferal $\delta^{13}C$ in Fig. 7). In theory [*Zeebe et al.*, 2017], an increase in the phase lag suggests an increase in the residence time oceanic carbon, either through a rise in the total carbon inventory or a drop in the supply and burial of carbon. The lengthening of the phase lag of the 405 ky cycle coincides with a large shift in the benthic foraminiferal $\delta^{13}C$ record across the OMT to more positive values, evidencing a structural relative increase in the supply of ^{13}C-depleted or drop in the burial of ^{13}C-enriched carbon. Reliable reconstructions of CO_2 are rare across the OMT (www.p-co2.org) and the OMT does not seem associated with a large change in

525 the depth of the Pacific calcite compensation depth [*Pälike et al.*, 2012]. Therefore,
526 additional constraints on atmospheric CO_2 concentrations and burial fluxes are
527 required to better understand the climatic/oceanographic mechanisms associated with
528 the increased phase lag.
529
530 **7. Conclusions**
531 We explore the application of $CaCO_3$ content (estimated from magnetic susceptibility
532 and shipboard coulometry) and benthic foraminiferal $\delta^{13}C$ records as tuning signals
533 for the OMT record at Site U1334 in the eastern equatorial Pacific. These two tunings
534 highlight the importance of carefully considering the implications of tuning choices
535 and assumptions when creating astronomical age models. Spreading rate histories
536 provide independent support for $CaCO_3$ tuned age model. This suggests that
537 lithological signals respond more directly (though still nonlinearly) to eccentricity
538 than the stable isotope signals, for which we find support for a delayed response to
539 astronomical climate forcing. Tuning to $CaCO_3$ provides a valuable method to better
540 understand the (lagged) response in benthic foraminiferal $\delta^{18}O$ and $\delta^{13}C$, which are
541 widely used and reproducible proxies for the global climate/cryosphere system and
542 (marine) carbon cycle. One important implication of the $CaCO_3$ age model is that 405
543 ky cycle in benthic $\delta^{13}C$ shows a distinct phase lag with respect to orbital eccentricity.
544 Lastly, the $CaCO_3$ age model for Site U1334 provides astronomically calibrated ages
545 for C6Bn.1n to C7n.1r. The polarity chron ages from the $CaCO_3$ tuned ages are
546 generally older by approximately 40 ky on average than those presented in the
547 GTS2012. We suggest that these updated early Miocene ages are incorporated in the
548 next version of the Geologic Time Scale.
549

Acknowledgements

This research used samples provided by the Integrated Ocean Drilling Program (IODP), collected by the staff, crew and scientists of IODP Expedition 320/321. We thank Dominika Kasjanuk, Arnold van Dijk, Maxim Krasnoperov and Jan Drenth for laboratory assistance. Linda Hinnov kindly provided her evolutive analysis MATLAB script. This research was supported by PalaeoClimate.Science (D.L.), NWO grant 865.10.001 (L.J.L), ERC grants 617462 (D.L.) and 259627 (A.S.), NERC grant NE/G014817 (B.S.W.), and a Marie Curie Career Integration Grant "ERAS". All data, on the preferred $CaCO_3$ tuned age model, can be downloaded from www.pangaea.de, or by following this link: https://doi.pangaea.de/10.1594/PANGAEA.885365 .

Figure Captions

Figure 1. Locations of ODP and IODP drill sites discussed in this study. Location of IODP Site U1334 with reference to ODP Sites 1264, 1218, 926, 929 and 1090.

Figure 2. Calibration between the shipboard magnetic susceptibility record and shipboard coulometric $CaCO_3$ measurements to estimate $CaCO_3$ content. (a) The magnetic susceptibility/$CaCO_3$ content record [*Pälike et al.*, 2010; *Westerhold et al.*, 2012a]. Green area indicates the 2σ uncertainty estimate of the coulometry measurements [*Pälike et al.*, 2010]. Red circles represent shipboard coulometric $CaCO_3$ values. **(b)** The relationship between coulometric $CaCO_3$ measurements and resampled magnetic susceptibility is calculated using ordinary least squares linear regression, and yields an R^2 value of 0.92.

Table 1. Comparison of magnetostratigraphic reversal ages. Chron boundary ages across the Oligocene Miocene Transition from the published literature and this study. Age differences with the GTS2012 age are presented in the lower part of the table. A: [*Lourens et al.*, 2004]; B: [*Hilgen et al.*, 2012; *Vandenberghe et al.*, 2012]; C: [*Billups et al.*, 2004]; D & E: [*Pälike et al.*, 2006b]; F: [*Liebrand et al.*, 2016]; G: [*Channell et al.*, 2013]; H & I: [this study].

Figure 3. Site U1334 datasets, evolutive spectra and power spectra against depth. **(a)** Magnetostratigraphy for Site U1334 [*Channell et al.*, 2013]. **(b)** The $CaCO_3$ content record. **(c)** The benthic foraminiferal $\delta^{18}O$ record. **(d)** The benthic foraminiferal $\delta^{13}C$ record. Dashed line marks the base of magnetochron C6Cn.2n; the boundary between the Oligocene and the Miocene. **(e)** Depth-evolutive FFT analysis and power spectra of the $CaCO_3$ content record, **(f)** the benthic foraminiferal $\delta^{18}O$ record, and **(g)** the benthic foraminiferal $\delta^{13}C$ record. All data is presented on the revised splice of *Westerhold et al.* [2012a].

Figure 4. Depth versus age relationships for the different age models for Site U1334. Magnetochron ages are based on GTS2012 [*Vandenberghe et al.*, 2012; *Hilgen et al.*, 2012], the initial age model (i.e., a third order polynomial through the GTS2012 ages), the $CaCO_3$ content age model and the $\delta^{13}C$ age model. Magnetochrons are plotted as colored circles.

Figure 5. **Implication of age models on time series analysis. (a-c)** Time-evolutive FFT analysis of $CaCO_3$ content on the initial magnetostratigraphic age model (i.e., a

599 third order polynomial), the $CaCO_3$ content tuned age model, and the $\delta^{13}C$ tuned age
600 model, respectively. **(d-f)** As in (a-c) but for benthic foraminiferal $\delta^{18}O$. **(g-i)** As in (a-
601 c) but for benthic foraminiferal $\delta^{13}C$. For all records, periodicities larger than 600 ky
602 are removed using a notch-filter. For panels b to i: coherence with, and phase
603 relationships to, eccentricity (La2011 solution) are depicted. All proxy data records
604 were multiplied by −1 before computing the phase estimates.
605
606 **Figure 6. Site U1334 $CaCO_3$ versus age. (a)** The $CaCO_3$ dataset and 405-ky and
607 ~110-ky Gaussian filters plotted on **(a)** the magnetostratigraphic age model, **(b)** the
608 $\delta^{13}C$ tuned age model, and **(c)** the $CaCO_3$ tuned age model. **(d)** Earth's orbital
609 eccentricity solution is plotted in grey [*Laskar et al.*, 2010, *Laskar et al.*, 2011]. Tie
610 points are represented by red dots and dashed lines. Gaussian filters were calculated
611 in AnalySeries [*Palliard et al.*, 1996] with the following settings: 405 ky – *f : 2.5 bw*
612 *0.8,* ~110 ky – *f : 10, bw : 3.* **(e)** Sedimentation rates are calculated using the $CaCO_3$
613 tuned age model.
614
615 **Figure 7**. **Site U1334 $\delta^{13}C$ versus age.** The $\delta^{13}C$ dataset and 405-ky and ~110-ky
616 Gaussian filters plotted on **(a)** the magnetostratigraphic age model, **(b)** the $CaCO_3$
617 tuned age model, and **(c)** the $\delta^{13}C$ tuned age model. **(d)** Earth's orbital eccentricity
618 solution is plotted in grey [*Laskar et al.*, 2010, *Laskar et al.*, 2011]. Tie points are
619 represented by red dots and dashed lines. Gaussian filters were calculated in
620 AnalySeries [*Palliard et al.*, 1996] with the following settings: 405 ky – *f : 2.5 bw*
621 *0.8,* ~110 ky – *f : 10, bw : 3.* **(e)** Sedimentation rates are calculated using the $\delta^{13}C$
622 tuned age model.
623

Table 2. Comparison of tuning methods and phase relationships. List of astronomically dated Oligocene-Miocene spanning record. Tuning signal (i.e., lithological or climatic proxy records) and target curves (i.e., astronomical solutions), and phase relationships to the target curves are compared. Please note: not all records span the same time interval, and that time-average, mid-phase estimates are given. A: [*Billups et al.*, 2004], B: [*Pälike et al.*, 2006a], C: [*Pälike et al.*, 2006b], D: [*Liebrand et al.*, 2016], for time-evolutive phase-estimates of benthic foraminiferal $\delta^{18}O$ with respect to eccentricity see [*Liebrand et al.*, 2017], E & F: [this study].

Figure 8. **Plate-pair spreading rates based on different age models.** Reduced-distance plots for the labeled plate pairs implied by **(a)** the GTS2012, **(b)** the $CaCO_3$ tuned age model and **(c)** the $\delta^{13}C$ tuned age model. Reduced distance is the full spreading distance (D) minus the age (A) times the labeled spreading rate (R, see y-axes). Distance scale is plotted inversely with spreading rate. This results in age errors that depart vertically from a straight line, when spreading rates are constant. Inset scale bar shows the vertical offset resulting from a 100-kyr change in a reversal age. Dashed horizontal lines are viewing aids to evaluate the prediction that constant spreading at the reduction rate R will produce a horizontal line. Error bars are 95% confidence. The $CaCO_3$ based age model **(b)** gives the simplest spreading rate history and represents the preferred tuning option.

References

Barckhausen, U., C. R. Ranero, S. C. Cande, M. Engels and W. Weinrebe (2008), Birth of an intraoceanic spreading center. *Geology*, *36*(10), 767-770.

649 Beddow, H. M., D. Liebrand, A. Sluijs, B. S. Wade, and L. J. Lourens (2016), Global
650 change across the Oligocene-Miocene transition: High-resolution stable isotope
651 records from IODP Site U1334 (equatorial Pacific Ocean), *Paleoceanography,*
652 *31, doi:10.1002/2015PA002820.*
653
654 Berner, R. A., A. C. Lasaga, and R. M. Garrels (1983), The carbonate-silicate
655 geochemical cycle and its effect on atmospheric carbon dioxide over the past
656 100 million years. *American Journal of Science, 283,* 641–683, doi:
657 10.2475/ajs.283.7.641.
658
659 Billups, K., H. Pälike, J. E. T. Channell, J. C. Zachos, and N. J. Shackleton (2004),
660 Astronomic calibration of the late Oligocene through early Miocene
661 geomagnetic polarity time scale, *Earth Planet. Sci. Lett*., *224*, 33–44,
662 doi:10.1016/j.epsl.2004.05.004.
663
664 Broecker, W. S. (1982), Glacial to interglacial changes in ocean chemistry, *Progress*
665 *in Oceanography*, 11, 2, 151-197.
666
667 Broecker, W. S., T-H Peng (1982), Tracers in the Sea, Lamont-Doherty Geological
668 Observatory, Columbia University.
669
670 Cande, S. C., and D. V. Kent (1992), A new geomagnetic polarity time scale for the
671 Late Cretaceous and Cenozoic, *J. Geophys. Res.*, *97*(B10), 13917-13951.
672

673 Cande, S. C., and J. M. Stock (2004), Pacific-Antarctic-Australia motion and the
674 formation of the Macquarie plate, *J. Geophys. Int.*, 157, 399-414.
675
676 Channell, J .E. T., C. Ohneiser, Y. Yamamoto, and M.S. Kesler (2013), Oligocene-
677 Miocene magnetic stratigraphy carried by biogenic magnetite at sites U1334
678 and U1335 (equatorial Pacific ocean) *Geochemistry, Geophysics, Geosystems,*
679 *14*(2) pp1525-2027doi:10.1029/2012GC004429.
680
681 Croon, M. B., S. C. Cande, and J. M. Stock (2008), Revised Pacific-Antarctic plate
682 motions and geophysics of the Menard Fracture Zone: *Geochemistry,*
683 *Geophysics, Geosystems*, v. 9, Q07001, doi:10.1029/2008GC002019.
684
685 DeConto, R.M., S. Galeotti, M. Pagani, D. Tracy, K. Schaefer, T. Zhang, D. Pollard,
686 and J.D. Beerling, (2012). Past extreme warming events linked to massive
687 carbon release from thawing permafrost. *Nature*, *484*(7392), p.87.
688
689 Diester-Haass, L., K. Billups, and K. Emeis (2011), Enhanced paleoproductivity
690 across the Oligocene/Miocene boundary as evidenced by benthic foraminiferal
691 accumulation rates. *Palaeogeography, Palaeoclimatology, Palaeoecology* 302,
692 464 - 473 doi:10.1016/j.palaeo.2011.02.006
693
694 Diester-Haass, L., K. Billups, I. Jacquemin, K.C. Emeis, V. Lefebvre and L. François,
695 (2013). Paleoproductivity during the middle Miocene carbon isotope events: A
696 data-model approach. *Paleoceanography*, *28*(2), 334-346.
697

698 Gradstein, F. M., J. G. Ogg, M. D. Schmitz and G. M. Ogg (2012), *The geologic time*
699 *scale 2012*.
700
701 Herbert, T. D (1994), Reading orbital signals distorted by sedimentation: models and
702 examples. *Orbital forcing and cyclic sequences*, 483-507.
703
704 Hilgen, F. J., L. J. Lourens, and J. A. Van Dam (2012), The Neogene Period. *The*
705 *geologic time scale*, *2*, 923-978.
706
707 Hodell, D. A., and F. Woodruff (1994), Variations in the strontium isotopic ratio of
708 seawater during the Miocene: Stratigraphic and geochemical implications.
709 *Paleoceanography* **9**, 405-426.
710
711 Hodell, D.A., C.D. Charles and F.J. Sierro (2001), Late Pleistocene evolution of the
712 ocean's carbonate system. *Earth and Planetary Science Letters*, *192*(2), pp.109-
713 124.
714
715 Holbourn, A., W. Kuhnt, J. T. Simo and Q. Li (2004), Middle Miocene isotope
716 stratigraphy and paleoceanographic evolution of the northwest and southwest
717 Australian margins (Wombat Plateau and Great Australian Bight).
718 *Palaeogeography, Palaeoclimatology, Palaeoecology*, *208*(1), 1-22.
719
720 Holbourn, A., W. Kuhnt, S. Clemens, W. Prell, and N. Andersen (2013), Middle to
721 late Miocene stepwise climate cooling: Evidence from a high-resolution deep-

water isotope curve spanning 8 million years, *Paleoceanography, 28*, doi:10.1002/2013PA002538.

Huybers, P., O. Aharonson, 2010. Orbital tuning, eccentricity, and the frequency modulation of climatic precession. Paleoceanography 25. doi:10.1029/2010PA001952

Hüsing, S. K., F. J. Hilgen, H. Abdul Aziz, and W. Krijgsman (2007), Completing the Neogene geological time scale between 8.5 and 12.5 Ma, *Earth and Planetary Science Letters*, *253*, 340-358.

Khider, D., S. Ahn, L.E. Lisiecki, C.E. Lawrence, M. Kienast, M., 2017. The role of uncertainty in estimating lead/lag relationships in marine sedimentary archives: A case study from the tropical Pacific. Paleoceanography 2016PA003057. doi:10.1002/2016PA003057

King, T. (1996). Quantifying nonlinearity and geometry in time series of climate. *Quaternary Science Reviews*, *15*(4), 247-266.

Krijgsman, W., F. J. Hilgen, I. Raffi, F. J. Sierro and D. S Wilson (1999), Chronology, causes and progression of the Messinian salinity crisis. *Nature*, *400*(6745), 652-655.

Kochhann, K. G., Holbourn, A., Kuhnt, W., Channell, J. E., Lyle, M., Shackford, J. K., Andersen, N. (2016). Eccentricity pacing of eastern equatorial Pacific

carbonate dissolution cycles during the Miocene Climatic Optimum. *Paleoceanography*, *31*(9), 1176-1192.

Laskar, J., P. Robutel, F. Joutel, M. Gastineau, A. C. M Correia, and B. Levrard (2004), A long-term numerical solution for the insolation quantities of the Earth. *Astronomy & Astrophysics*, *428*(1), 261-285.

Laskar, J., A. Fienga, M. Gastineau, and H. Manche (2011a), La2010: A new orbital solution for the long term motion of the Earth, *Astronomy and Astrophysics*, *532*(A89).

Laskar, J., M. Gastineau, J.-B. Delisle, A. Farrés, and A. Fienga (2011b), Strong chaos induced by close encounters with Ceres and Vesta, *Astronomy and Astrophysics*, *532*(L4), 1-4.

Laurin, J., B. Růžek, M. Giorgioni, (2017). Orbital signals in carbon isotopes: phase distortion as a signature of the carbon cycle. Paleoceanography 2017PA003143. doi:10.1002/2017PA003143

Liebrand, D., L. Lourens, D. A. Hodell, B de. Boer, R. S. W. van der Wal, and H. Pälike (2011), Antarctic ice sheet and oceanographic response to eccentricity forcing in the early Miocene. *Climates of the past, 7*, pp 869 - 880.

Liebrand, D., H. M. Beddow, L. J. Lourens, H. Pälike, I. Raffi, S. M. Bohaty, F. J. Hilgen, Mischa J. M. Saes., P.A. Wilson, A. E. van Dijk, D. A. Hodell, D.

Kroon., C. E. Huck and S. J. Batenburg (2016). Cyclostratigraphy and eccentricity tuning of the early Oligocene through early Miocene (30.1-17.1 Ma): Cibicides mundulus stable oxygen and carbon isotope records from Walvis Ridge Site 1264. *Earth and Planetary Science Letters, 450*, 392-405.

Liebrand, D., A.T.M. de Bakker, H.M. Beddow, P.A. Wilson, S.M. Bohaty, G. Ruessink, H. Pälike, S.J. Batenburg, F.J. Hilgen, D.A. Hodell, C.E. Huck, D. Kroon, I. Raffi, M.J.M. Saes, A.E. van Dijk, and L.J. Lourens, (2017). Evolution of the early Antarctic ice ages. *Proceedings of the National Academy of Sciences of the United States of America*, *114(15)*, 3867-3872.

Littler, K., U. Röhl, T. Westerhold, and J.C. Zachos (2014). A high-resolution benthic stable-isotope record for the South Atlantic: Implications for orbital-scale changes in Late Paleocene–Early Eocene climate and carbon cycling. *Earth and Planetary Science Letters*, *401*, 18-30.

Lonsdale, P., (2005), Creation of the Cocos and Nazca plates by fission of the Farallon plate: *Tectonophysics*, v. 404, p. 237–264, doi: 10.1016/ j.tecto.2005.05.011.

Lourens, L. J., F. J. Hilgen, N. J. Shackleton, J. Laskar and D. Wilson (2004),'Chapter 21: The Neogene Period'. In: Gradstein, F., Ogg, J. and Smith,A., (eds).,*A Geologic Time Scale 2004*, Cambridge University Press, Cambridge, pp. 409-440.

797 Ma, W., J. Tian, Q. Li, and P. Wang (2011), Simulation of long eccentricity (400-kyr)
798 cycle in ocean carbon reservoir during Miocene Climate Optimum: Weathering
799 and nutrient response to orbital change, *Geophys. Res. Lett., 38*, L10701,
800 doi:10.1029/2011GL047680.
801
802 Paillard, D., L. Labeyrie, and P. Yiou (1996), Macintosh program performs time‐
803 series analysis, *Eos Trans. AGU*, *77*, 379, doi:10.1029/96EO00259.
804
805 Pälike, H., J. Frazier, and J.C. Zachos (2006a), Extended orbitally forced
806 palaeoclimatic records from the equatorial Atlantic Ceara Rise. *Quaternary*
807 *Science Reviews,* 25, 3138–3149.
808
809 Pälike, H., R. N. Norris, J. Herrle, P. A. Wilson, H. K. Coxall, C. H. Lear, N. J.
810 Shackleton, A. K. Tripati, and B. S. Wade (2006b), The heartbeat of the
811 Oligocene climate system, *Science, 314*, 1894–1898, doi:10.1126/
812 science.1133822.
813
814 Pälike, H., M. W. Lyle, H. Nishi, I. Raffi, K. Gamage, A. Klaus and the Expedition
815 320/321 Scientists (2010), *Proceedings of the Integrated Ocean Drilling*
816 *Program*, Volume 320/321. Tokyo (Integrated Ocean Drilling Program
817 Management International, Inc.).
818
819 Pälike, H., M. W. Lyle, H. Nishi, I. Raffi, A. Ridgewell, K. Gamage, et al (2012), A
820 Cenozoic record of the equatorial Pacific carbonate compensation depth,
821 *Nature*, *488*(7413), 609-614.

Shackleton, N . J. (1977), Carbon-13 in Uvigerina: Tropical rain forest history and the equatorial Pacific carbonate dissolution cycles, in *The Fate of Fossil Fuel CO_2 in the Oceans*, edited by N.R. Andersen and A. Malahoff, 401-427, Plenum, New York,

Shackleton, N.J., T.K. Hagelberg, S.J. Crowhurst, 1995. Evaluating the success of astronomical tuning: Pitfalls of using coherence as a criterion for assessing pre-Pleistocene timescales. Paleoceanography 10, 693–697. doi:10.1029/95PA01454

Shackleton, N. J., S. J. Crowhurst, G. P. Weedon, and J. Laskar (1999), Astronomical Calibration of Oligocene-Miocene Time, *Philosophical Transactions: Mathematical, Physical and Engineering Sciences*, *357*(1757), 1907-1929.

Shackleton, N.J., M. A. Hall, I. Raffi, L. Tauxe, and J. C. Zachos (2000), Astronomical calibration age for the Oligocene/Miocene boundary. *Geology 28* (5), 447–450.

Vandenberghe, N., F. J. Hilgen, and R. P. Speijer (2012), The paleogene period. *The geologic time scale*, *2012*, 855-921.

Westerhold, T., et al. (2012a), Revised composite depth scales and integration of IODP Sites U1331–U1334 and ODP Sites 1218–1220, in *Proceedings of the*

Integrated Ocean Drilling Program, vol. 320/321, edited by H. Pälike et al., Integ. Ocean Drill. Progr. Manage. Int., College Station, Tex.

Westerhold, T., U. Röhl and J. Laskar (2012b), Time scale controversy: Accurate orbital calibration of the early Paleogene. *Geochemistry, Geophysics, Geosystems*, *13*(6).

Westerhold, T., Röhl, U., Frederichs, T., Agnini, C., Raffi, I., Zachos, J. C., and Wilkens, R. H. (2017). Astronomical Calibration of the Ypresian Time Scale: Implications for Seafloor Spreading Rates and the Chaotic Behaviour of the Solar System?, Clim. Past Discuss., doi:10.5194/cp-2017-15.

Wilson, D. S. (1988). Tectonic history of the Juan de Fuca ridge over the last 40 million years. *Journal of Geophysical Research: Solid Earth (1978–2012)*, *93*(B10), 11863-11876.

Wilson, D. S. (1993), Confirmation of the astronomical calibration of the magnetic polarity time scale from rates of sea-floor spreading, *Nature, 364*, 788-790.

Zachos, J. C., N. J. Shackleton, J. S. Revenaugh, H. Pälike, and B. P. Flower (2001), Climate response to orbital forcing across the Oligocene – Miocene boundary, *Science* 292, 274– 278.

869 Zeebe, R. E., T. Westerhold, K. Littler, J. C. Zachos (2017), Orbital forcing of the
870 Paleocene and Eocene carbon cycle, *Paleoceanography, 32,* 440–465,
871 doi:10.1002/2016PA003054.
872
873 Zeeden, C., F. J. Hilgen, S. K. Hüsing, and L. J. Lourens (2014), The Miocene
874 astronomical time scale 9–12 Ma: new constraints on tidal dissipation and their
875 implications for paleoclimatic investigations. *Paleoceanography*, *29*(4), 296-
876 307.

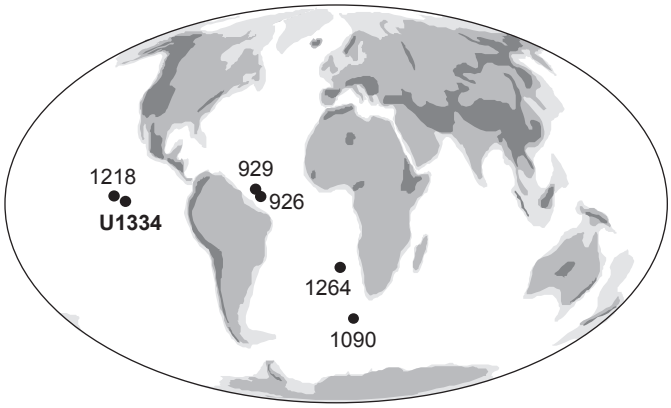
1218
U1334
929
926
1264
1090

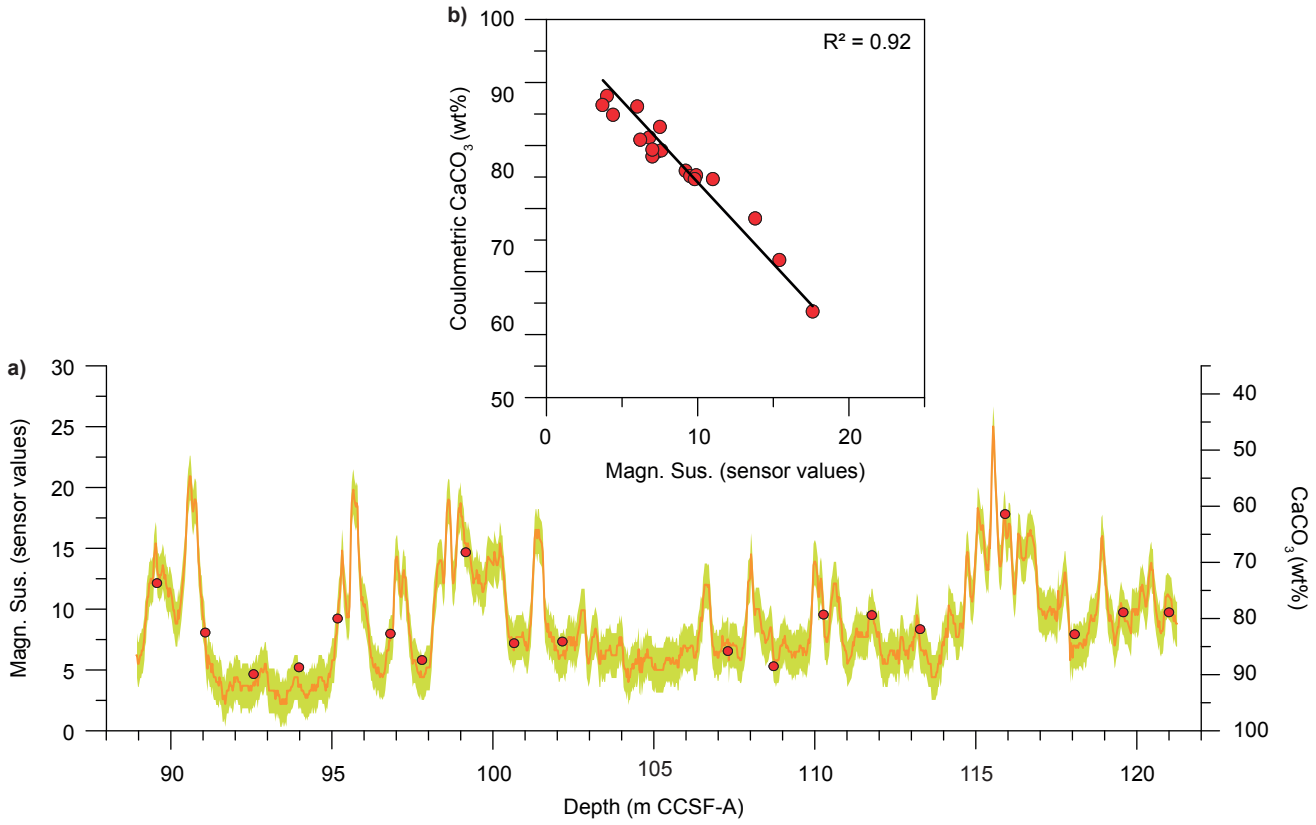
b)
R² = 0.92
Coulometric CaCO3 (wt%)
Magn. Sus. (sensor values)
a)
Magn. Sus. (sensor values)
CaCO3 (wt%)
Depth (m CCSF-A)

Table 1

Chron	A: Age GTS2004 (Ma)	B: Age GTS2012 (Ma)	C: 1090 Tuned age (Ma)	D: 1218 Manual tuned age (Ma)	E: 1218 Auto tuned age (Ma)	F: 1264 Mid tuned age (Ma)	G: U1334 Depth CCSF-A (m)	H: U1334 CaCO3 tuned age (Ma)	I: U1334 δ13C tuned age (Ma)
C6Bn.1n (o)	21.936	21.936	21.991	22.010	21.998		89.17	21.985	22.115
C6Bn.1r (o)	21.992	21.992	22.034	22.056	22.062		89.79	22.042	22.165
C6Bn.2n (o)	22.268	22.268	22.291	22.318	22.299	22.300	94.72	22.342	22.473
C6Br (o)	22.564	22.564	22.593	22.595	22.588	22.608	98.26	22.621	22.697
C6Cn.1n (o)	22.754	22.754	22.772	22.689	22.685	22.760	100.00	22.792	22.809
C6Cn.1r (o)	22.902	22.902	22.931	22.852	22.854	22.944	102.50	22.973	22.970
C6Cn.2n (o)	23.030	23.030	23.033	23.024	23.026	23.052	103.96	23.040	23.053
C6Cn.2r (o)	23.249	23.233	23.237	23.233	23.278	23.247	107.50	23.212	23.211
C6Cn.3n (o)	23.375	23.295	23.299	23.295	23.340	23.332	108.68	23.318	23.286
C6Cr (o)	24.044	23.962	23.988	23.962	24.022		119.10	24.025	24.026
C7n.1n (o)	24.102	24.000	24.013	24.000	24.062		119.58	24.061	24.066
C7n.1r (o)	24.163	24.109	24.138	24.109	24.147		120.76	24.124	24.161

(continued)

Chron	Δ B−C Age (ky)	Δ B−D Age (ky)	Δ B−E Age (ky)	Δ B−F Age (ky)	Δ B−H Age (ky)	Δ B−I Age (ky)
C6Bn.1n (o)	-55	-74	-62		-49	-179
C6Bn.1r (o)	-42	-64	-70		-50	-173
C6Bn.2n (o)	-23	-50	-31	-32	-74	-205
C6Br (o)	-29	-31	-24	-44	-57	-133
C6Cn.1n (o)	-18	65	69	-6	-38	-55
C6Cn.1r (o)	-29	50	48	-42	-71	-68
C6Cn.2n (o)	-3	6	4	-22	-10	-23
C6Cn.2r (o)	-4	0	-45	-14	21	22
C6Cn.3n (o)	-4	0	-45	-37	-23	9
C6Cr (o)	-26	0	-60		-63	-64
C7n.1n (o)	-13	0	-62		-61	-66
C7n.1r (o)	-29	0	-38		-15	-52

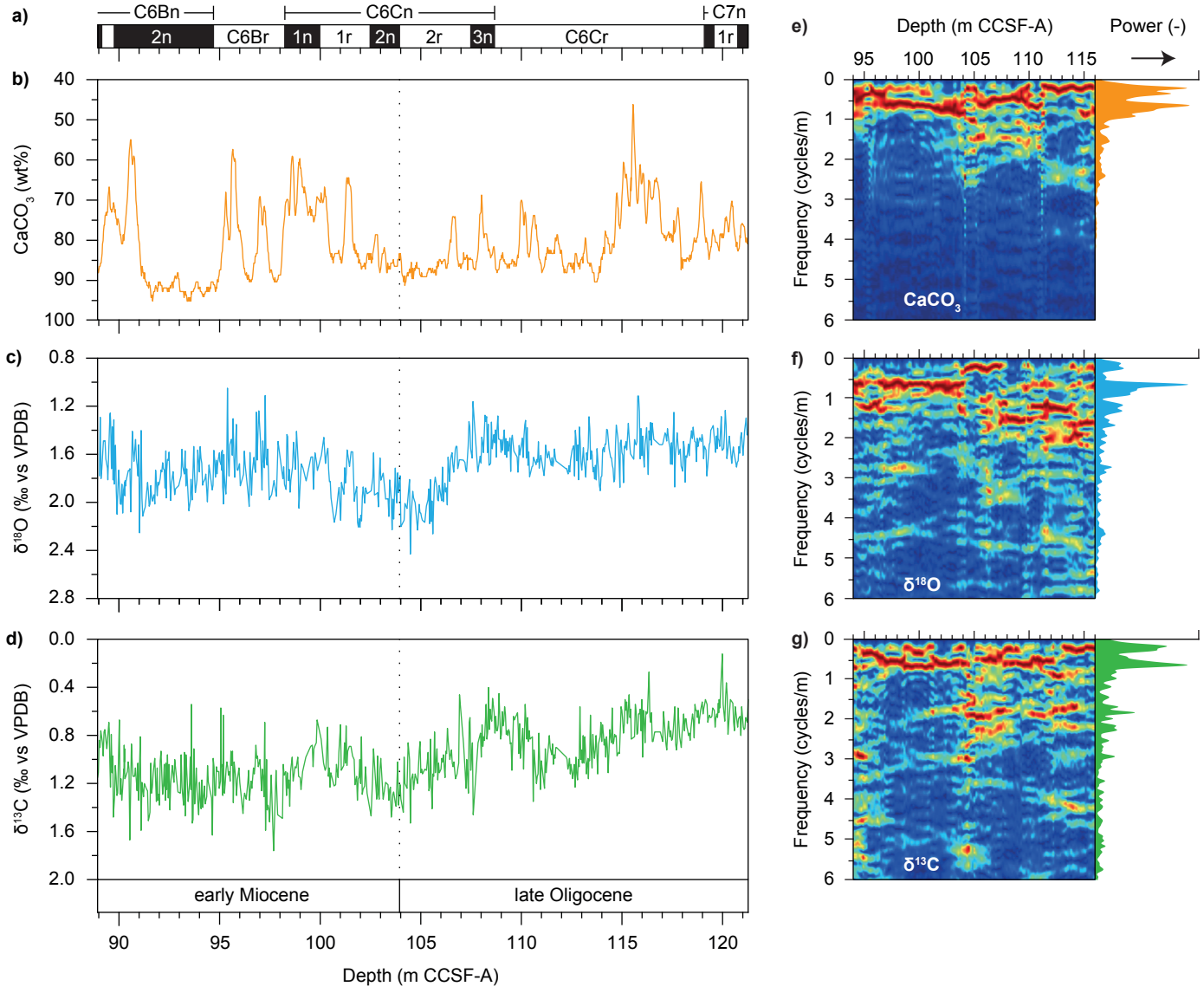
a)
C6Bn
C6Cn
C7n
2n
C6Br
1n
1r
2n
2r
3n
C6Cr
1r
b)
CaCO3 (wt%)
c)
δ18O (‰ vs VPDB)
d)
δ13C (‰ vs VPDB)
early Miocene
late Oligocene
Depth (m CCSF-A)
e)
Depth (m CCSF-A)
Power (-)
Frequency (cycles/m)
CaCO3
f)
δ18O
g)
δ13C

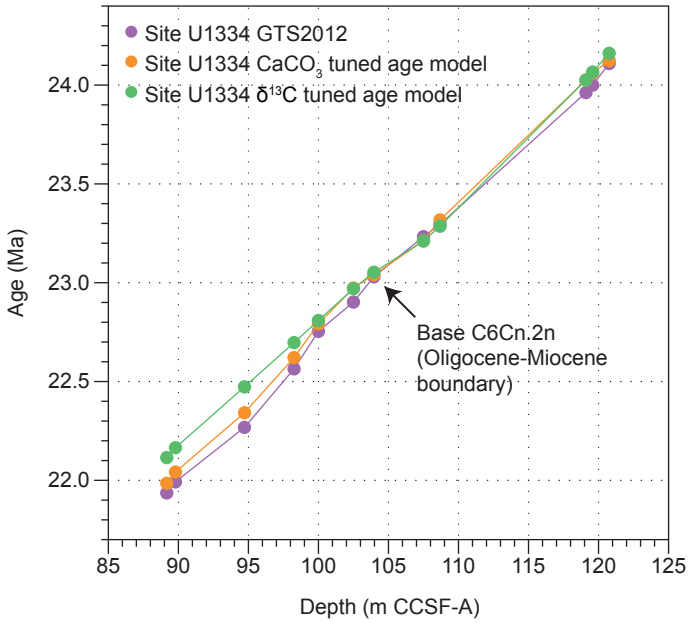
Site U1334 GTS2012
Site U1334 CaCO3 tuned age model
Site U1334 δ13C tuned age model
Base C6Cn.2n
(Oligocene-Miocene
boundary)
Age (Ma)
Depth (m CCSF-A)
24.0
23.5
23.0
22.5
22.0
85
90
95
100
105
110
115
120
125

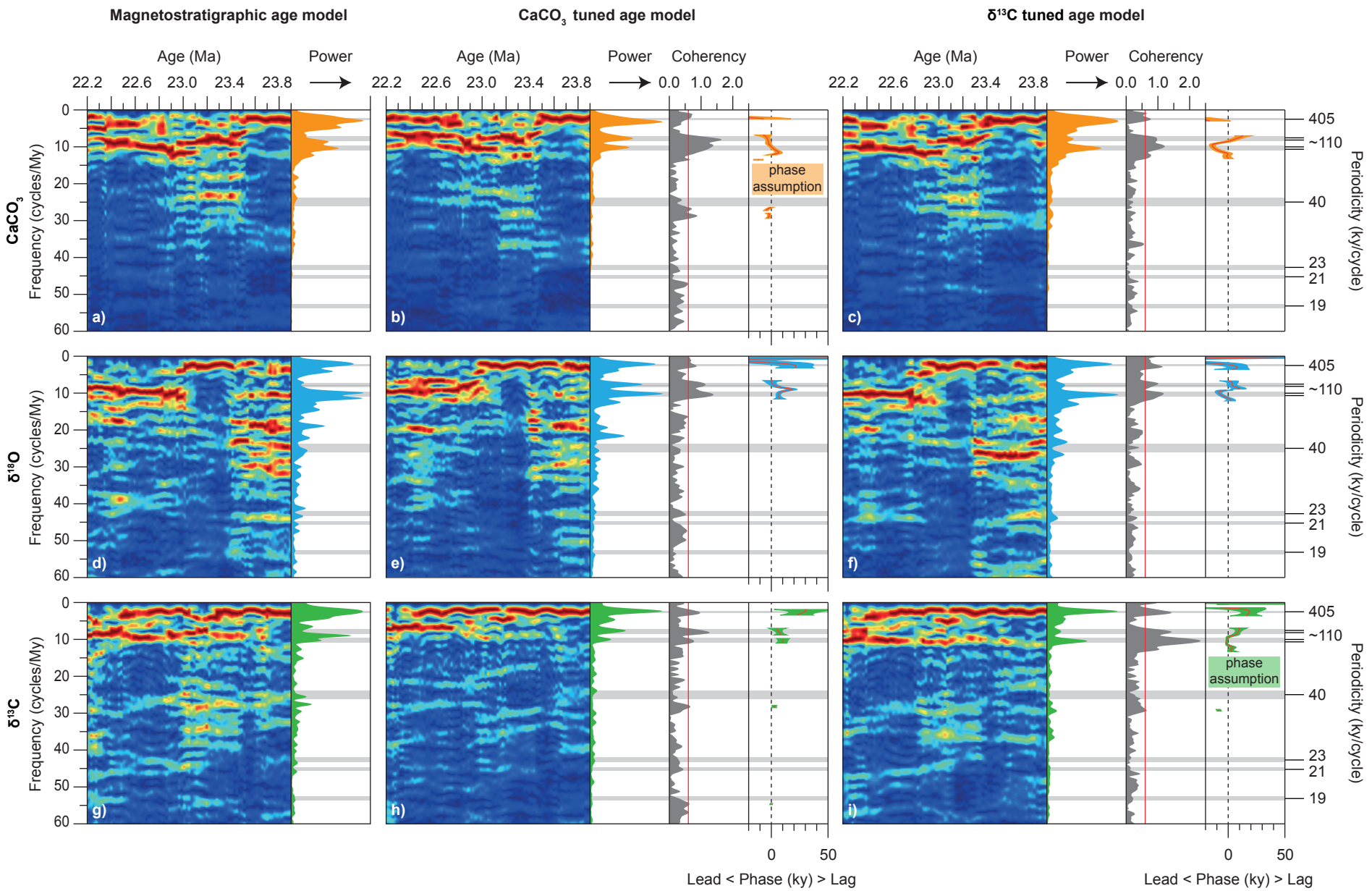
Magnetostratigraphic age model
CaCO3 tuned age model
δ13C tuned age model
Age (Ma)
Power
Coherency
22.2
22.6
23.0
23.4
23.8
0.0
1.0
2.0
CaCO3
δ18O
δ13C
Frequency (cycles/My)
Periodicity (ky/cycle)
405
~110
40
23
21
19
phase assumption
a)
b)
c)
d)
e)
f)
g)
h)
i)
0
50
Lead < Phase (ky) > Lag

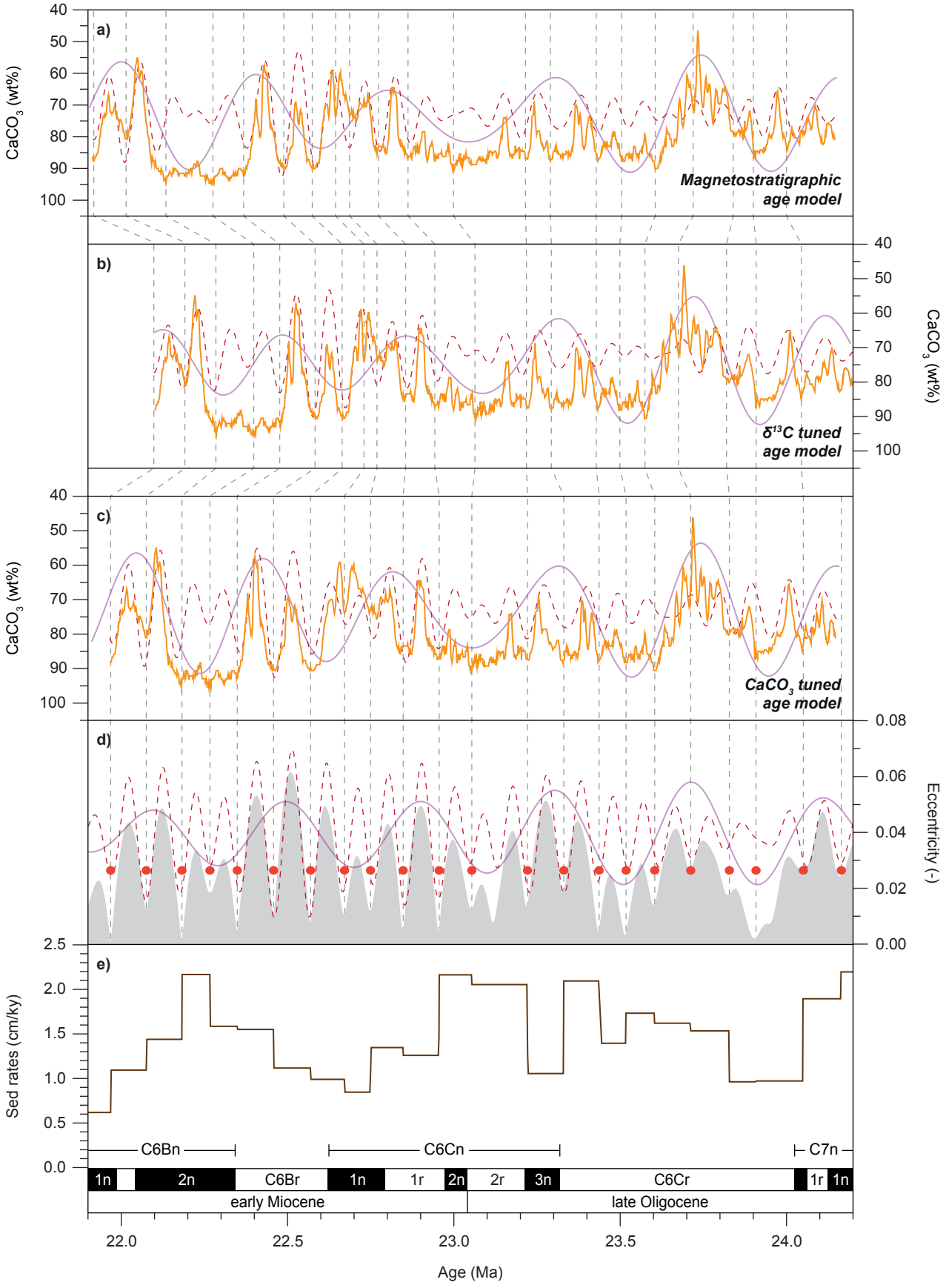
a)
Magnetostratigraphic age model
b)
δ13C tuned age model
c)
CaCO3 tuned age model
d)
e)
CaCO3 (wt%)
Eccentricity (-)
Sed rates (cm/ky)
C6Bn
C6Cn
C7n
1n
2n
C6Br
1n
1r
2n
2r
3n
C6Cr
1r
1n
early Miocene
late Oligocene
Age (Ma)

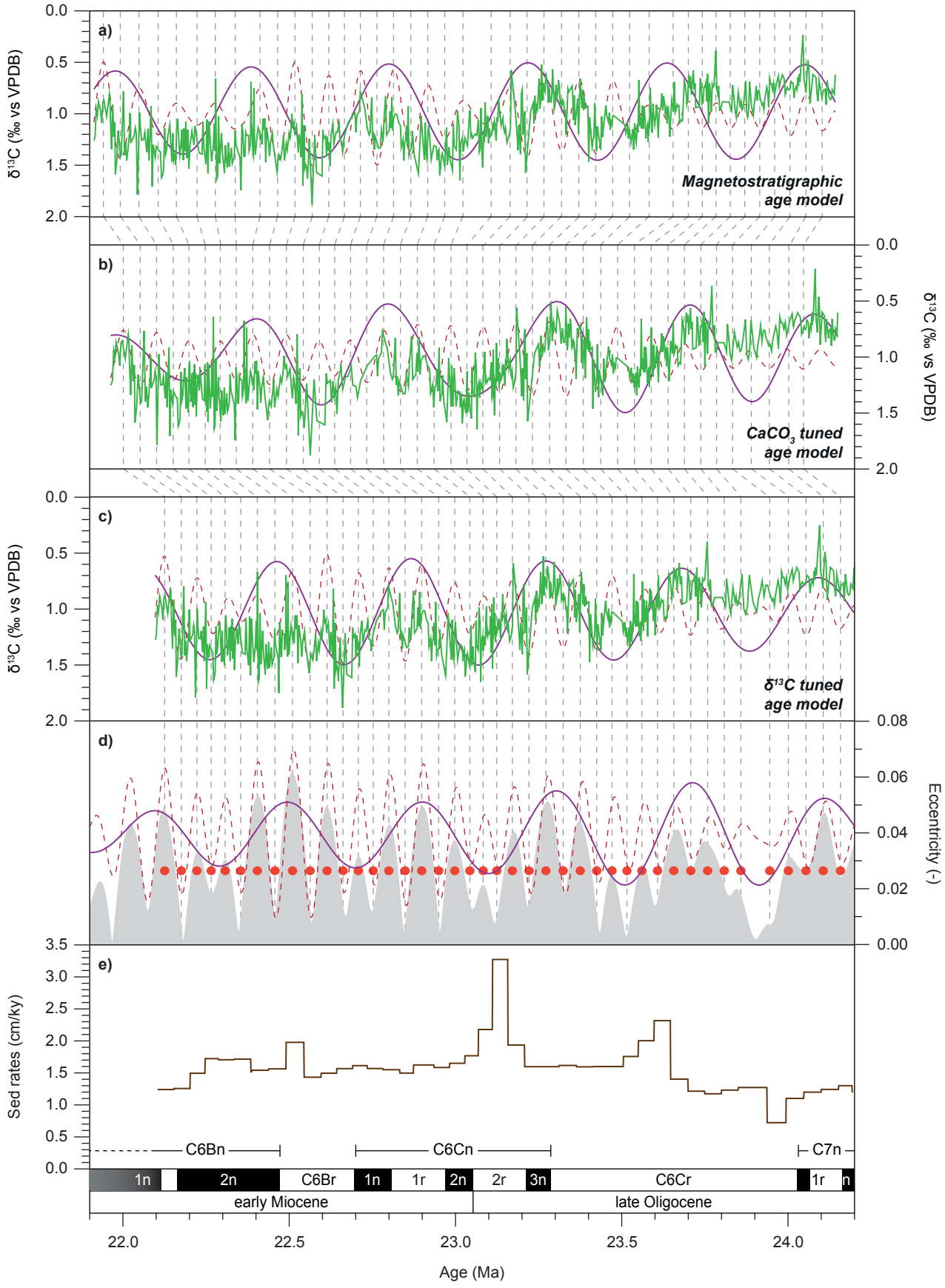
a)
b)
c)
d)
e)
δ13C (‰ vs VPDB)
Magnetostratigraphic age model
CaCO3 tuned age model
δ13C tuned age model
Eccentricity (-)
Sed rates (cm/ky)
C6Bn
C6Cn
C7n
1n
2n
C6Br
1n
1r
2n
2r
3n
C6Cr
1r
n
early Miocene
late Oligocene
Age (Ma)
22.0
22.5
23.0
23.5
24.0

Table 2

Site	Tuning signal	Tuning target	Age range	Lead(−)/ Lag(+) 405 ky $CaCO_3$ content	Lead(−)/ Lag(+) ~110 ky $CaCO_3$ content	Lead(−)/ Lag(+) 405 ky $\delta^{18}O$	Lead(−)/ Lag(+) ~110 ky $\delta^{18}O$	Lead(−)/ Lag(+) 405 ky $\delta^{13}C$	Lead(−)/ Lag(+) ~110 ky $\delta^{13}C$
A: 1090	Benthic foram. $\delta^{18}O$	E/O/P (mainly obliquity)	24–20 Ma	-	-	In phase	+5 ky	+25 ky	+10 ky
B: 926/929	$CaCO_3$ content*	E/O/P (mainly obliquity)	26–17 Ma	-	-	+10 ky	+25 ky	+35 ky	+28 ky
C: 1218	Benthic foram. $\delta^{13}C$	E/O/P (mainly eccentricity)	34–22 Ma	-	-	+8 ky	~In phase	+25 ky	~In phase
D: 1264	$CaCO_3$ content**	Eccentricity	30–17 Ma	Unstable phase	In phase	−14 ky	+12 ky	+36 ky	+12 ky
E: U1334	$CaCO_3$ content***	Eccentricity	24–22 Ma	+6 ky	In phase	+21 ky	+9 ky	+29 ky	+9 ky
F: U1334	Benthic foram. $\delta^{13}C$	Eccentricity	24–22 Ma	−24 ky	−7 ky	−4 ky	In phase	+19 ky	~In phase

*magnetic susceptibility and color reflectance
**natural logarithm of (X-ray fluorescence) Ca over Fe counts
***magnetic susceptibility

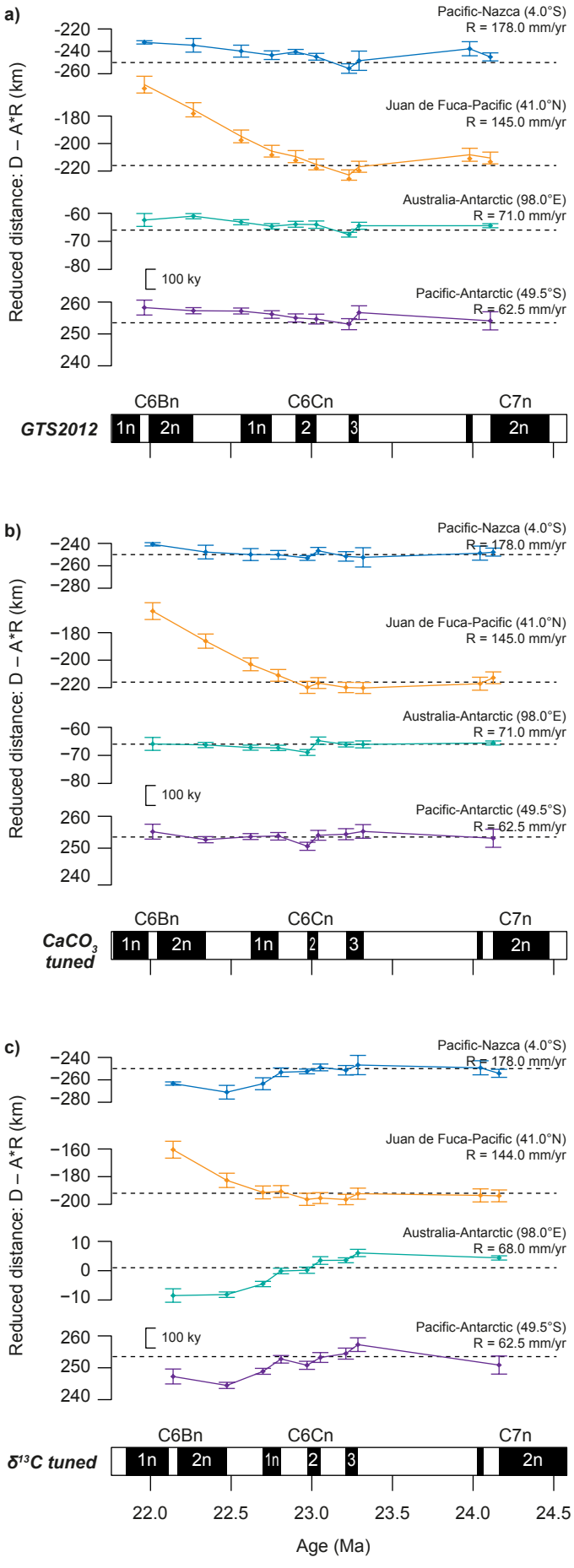
a)
Reduced distance: D – A*R (km)
Pacific-Nazca (4.0°S)
R = 178.0 mm/yr
Juan de Fuca-Pacific (41.0°N)
R = 145.0 mm/yr
Australia-Antarctic (98.0°E)
R = 71.0 mm/yr
Pacific-Antarctic (49.5°S)
R = 62.5 mm/yr
100 ky
C6Bn
C6Cn
C7n
GTS2012
1n
2n
2
3
b)
CaCO3 tuned
c)
Pacific-Nazca (4.0°S)
R = 178.0 mm/yr
Juan de Fuca-Pacific (41.0°N)
R = 144.0 mm/yr
Australia-Antarctic (98.0°E)
R = 68.0 mm/yr
Pacific-Antarctic (49.5°S)
R = 62.5 mm/yr
δ13C tuned
22.0
22.5
23.0
23.5
24.0
24.5
Age (Ma)